



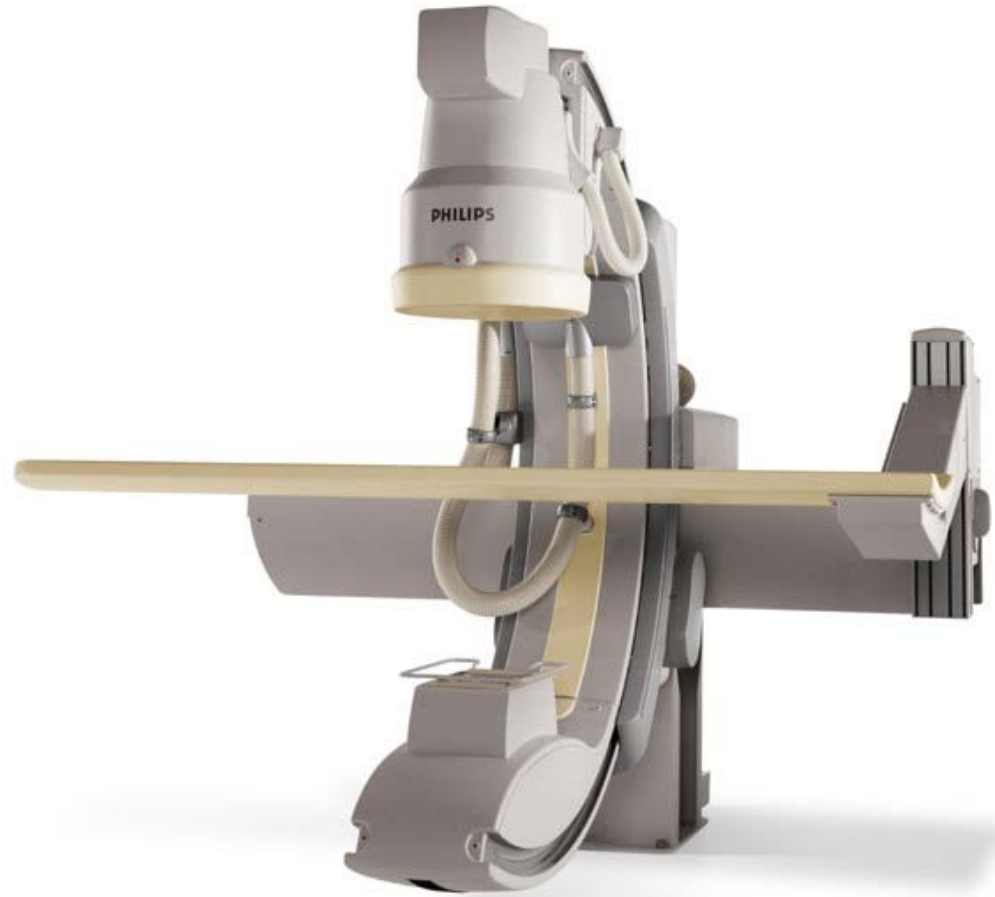
*X-ray diagnostics and
Computed tomography*





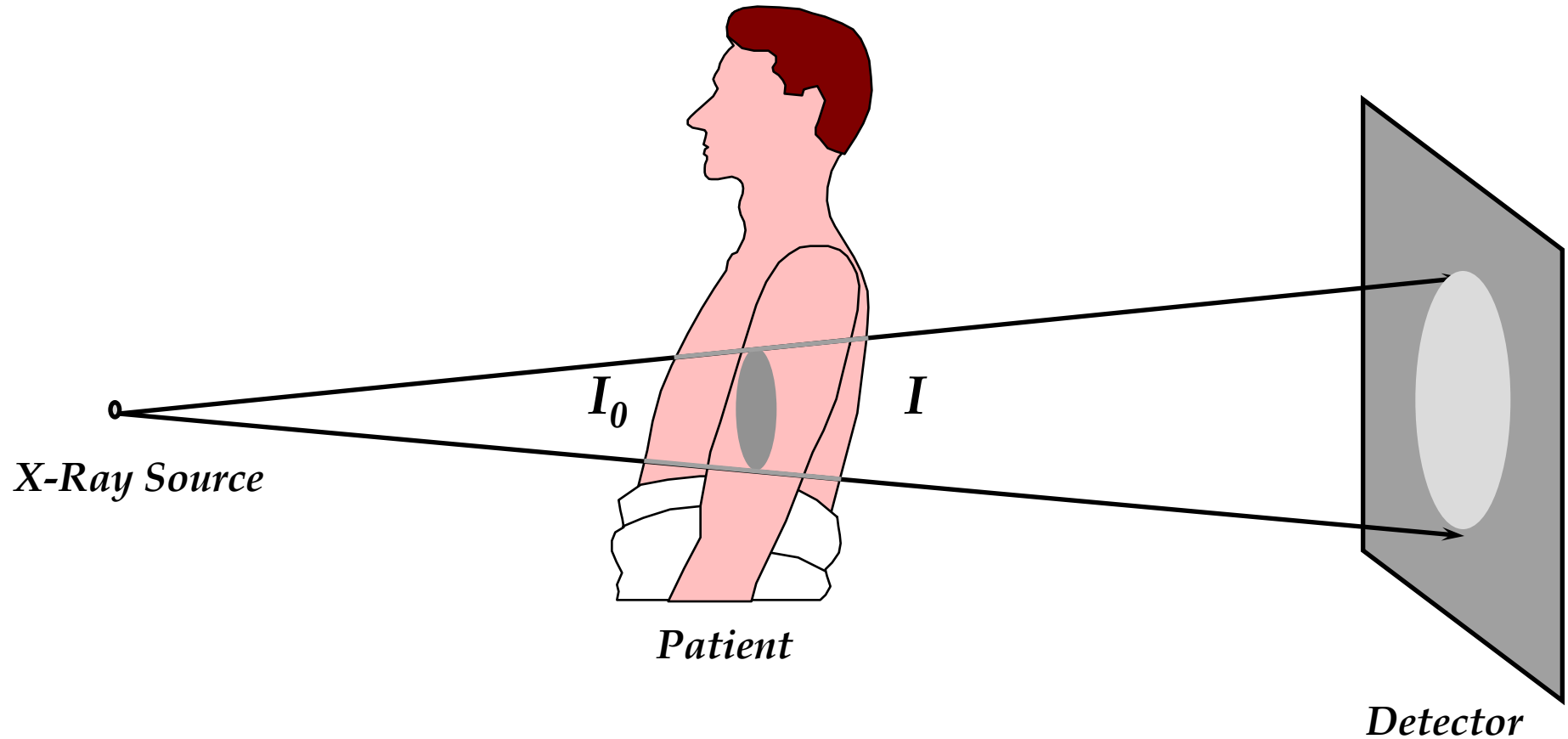
15th century head examination

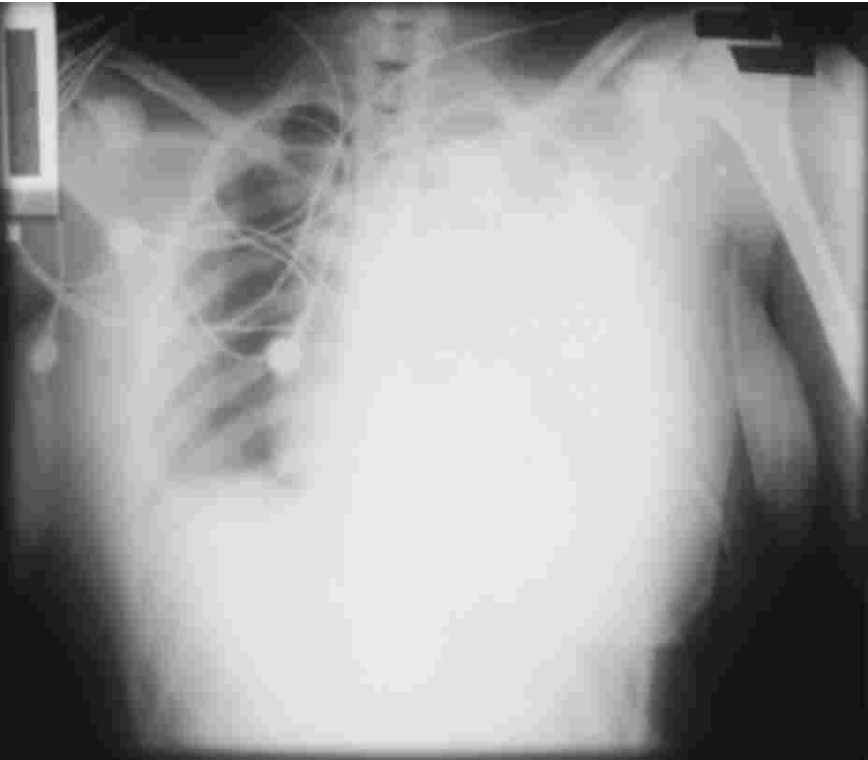






Projection Imaging with X Rays



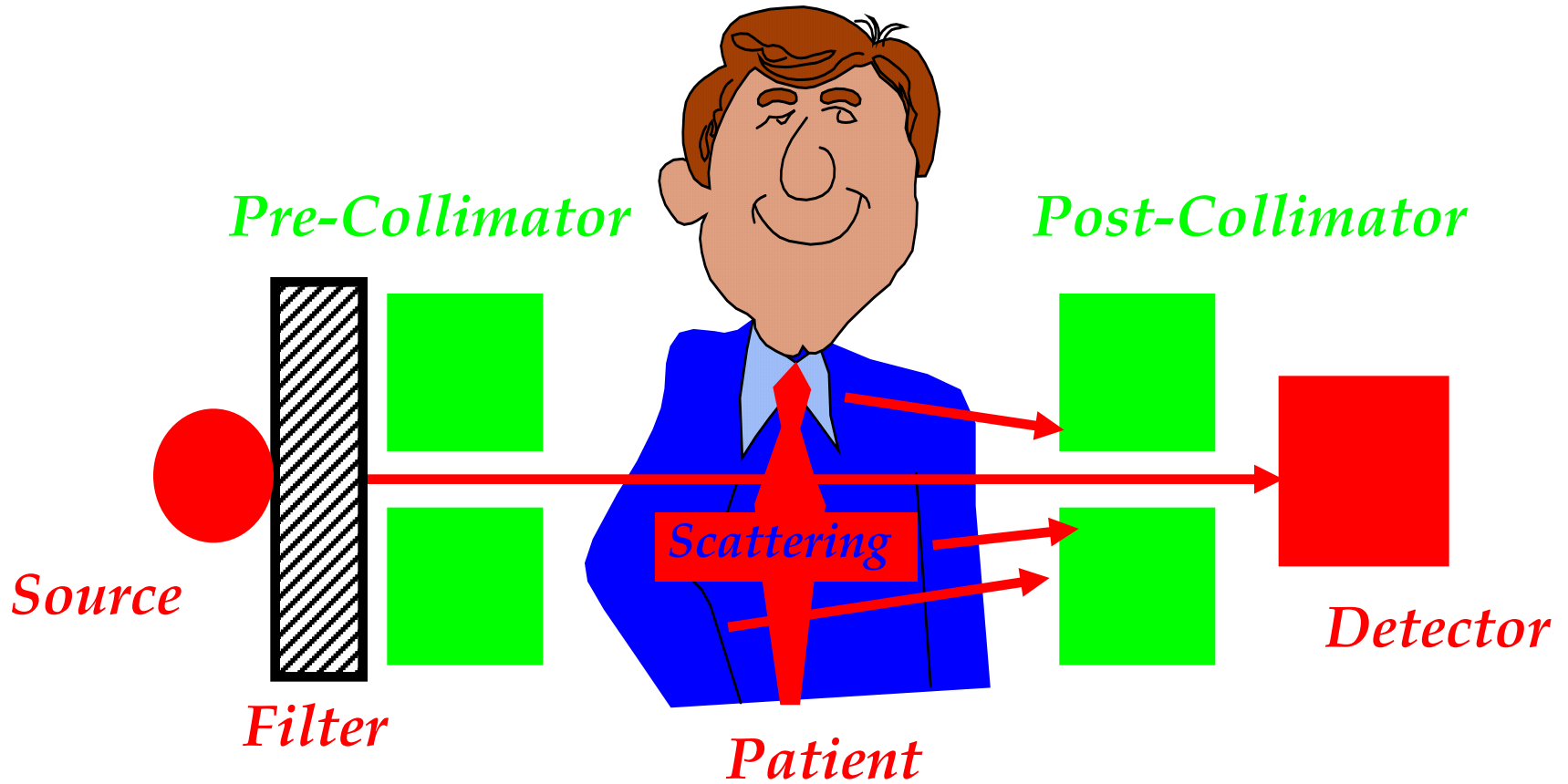


Chest X-Ray

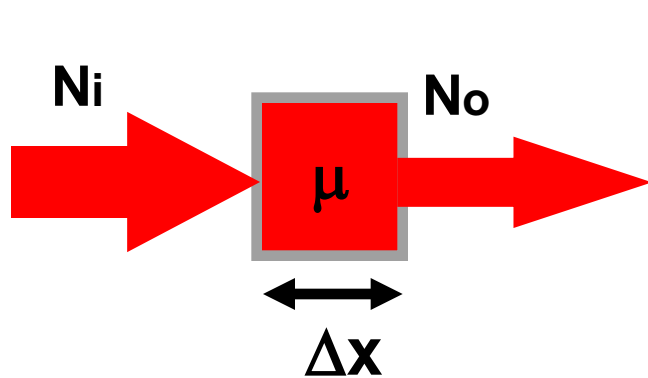
This frontal chest radiograph demonstrates a dense (radio-opaque) left lung field consistent with a hemothorax in a patient with a gunshot wound to the chest.



Data Acquisition System (DAS)

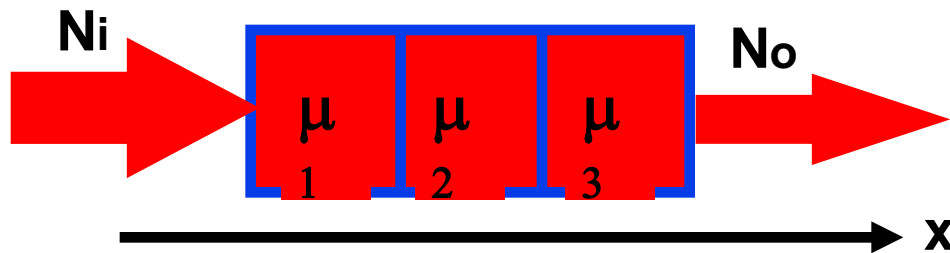


Exponential Attenuation of X-ray

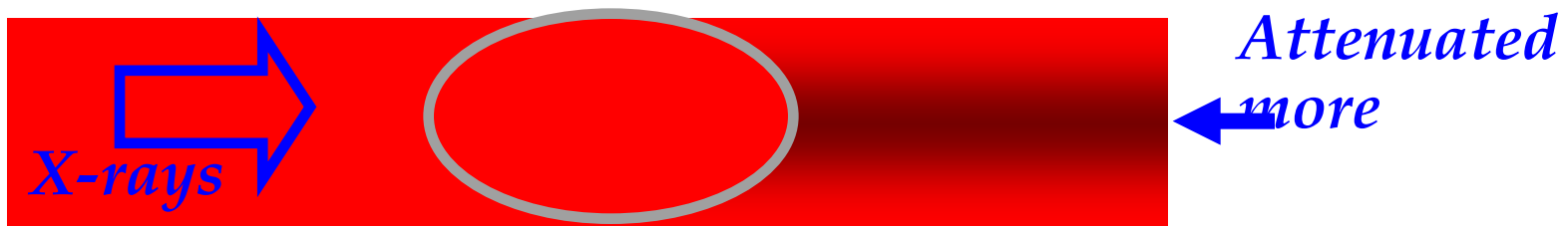


$$N_o = N_i e^{-\mu \Delta x}$$

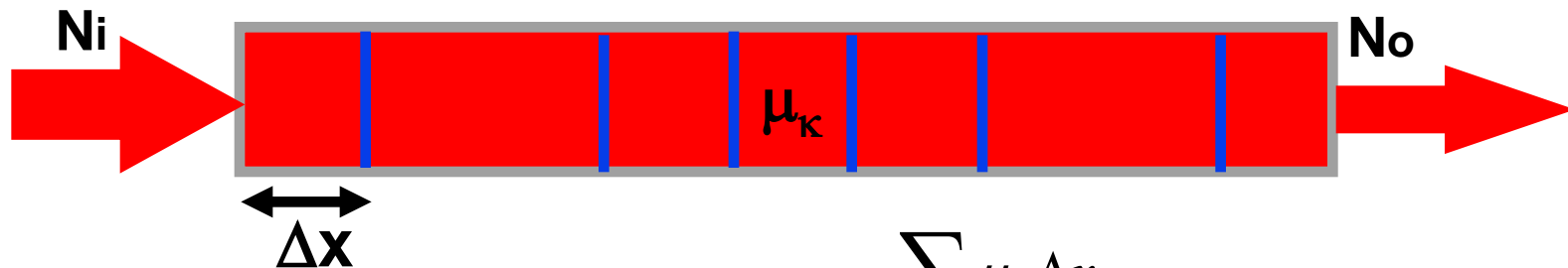
N_i : input intensity of X-ray
 N_o : output intensity of X-ray
 μ : linear X-ray attenuation



$$N_o = N_i e^{-(\mu_1 + \mu_2 + \mu_3) \Delta x}$$



Ray-Sum of X-ray Attenuation



$$N_o = N_i e^{-\sum_k \mu_k \Delta x}$$

Ray-sum

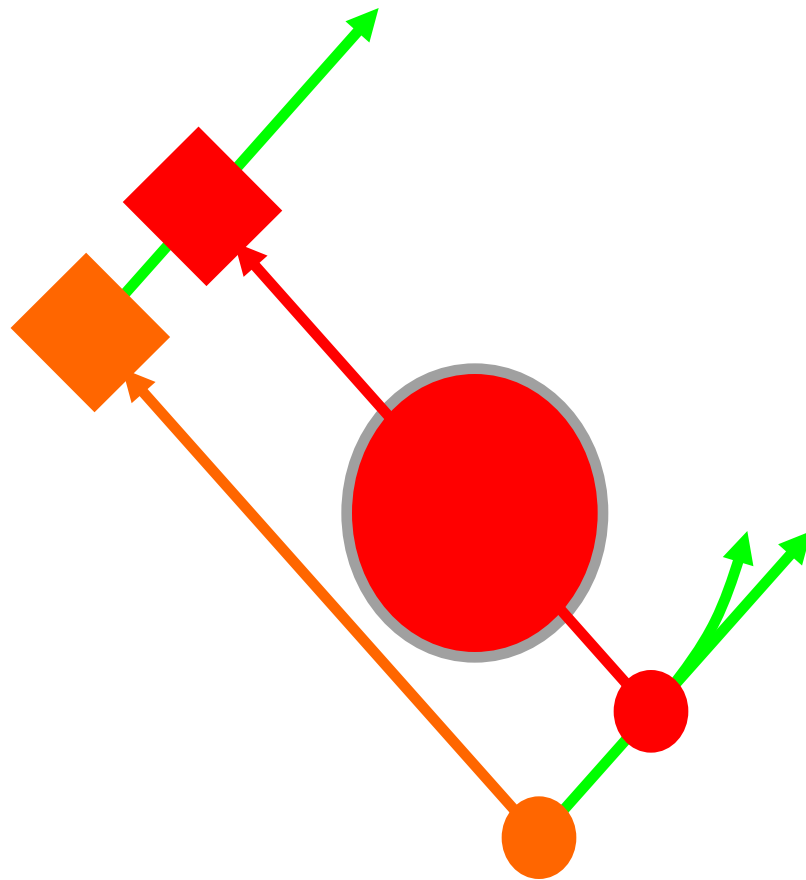
$$\sum_k \mu_k \Delta x = \ln \frac{N_i}{N_o}$$

Line integral

$$\int_{-\infty}^{\infty} \mu(x) dx = \ln \frac{N_i}{N_o}$$



First Generation

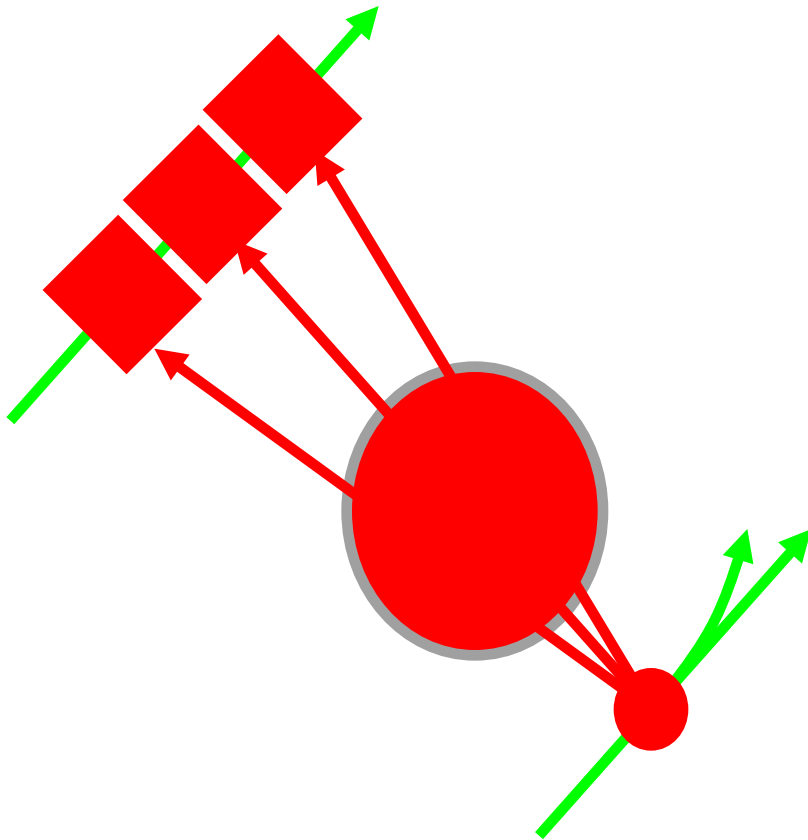


**One detector
Translation-rotation
Parallel-beam**





Second Generation

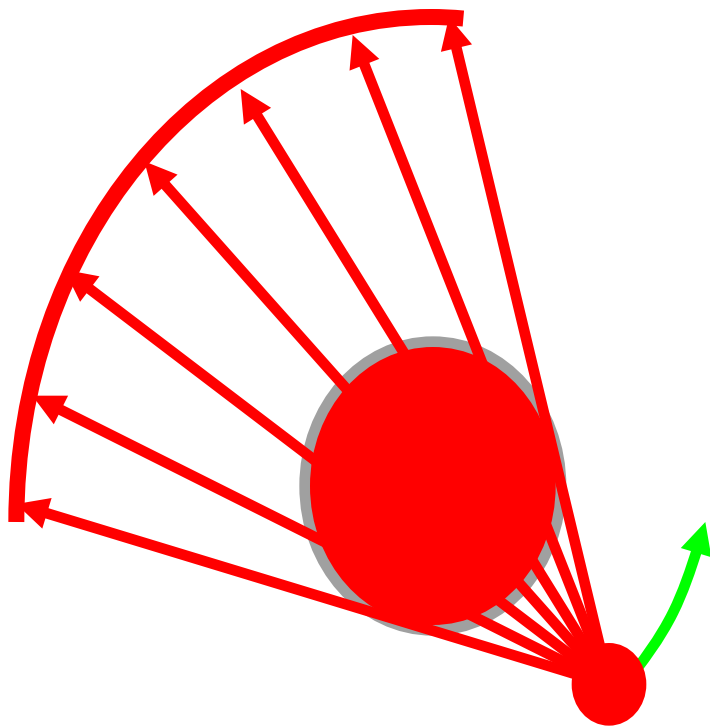


**Multiple detectors
Translation-rotation
Small fan-beam**





Third Generation

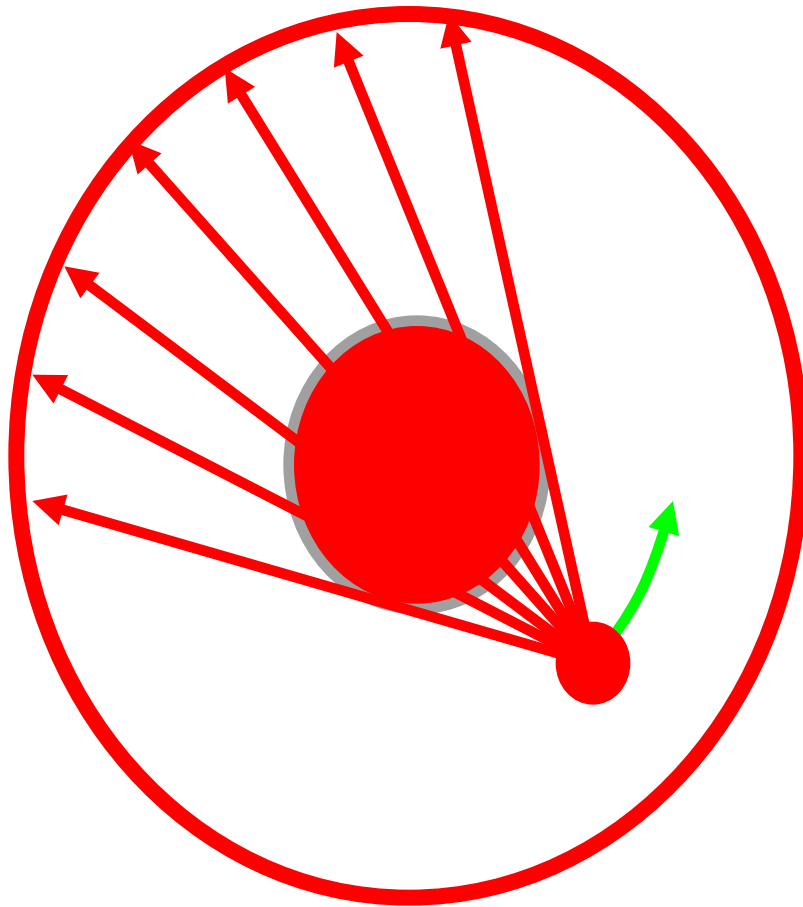


Multiple detectors
Translation-rotation
Large fan-beam





Fourth Generation

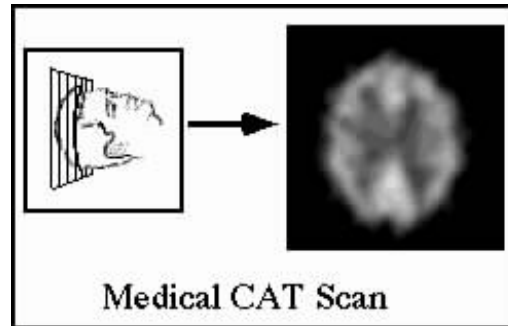


Detector ring
Source-rotation
Large fan-beam





A Little Bit History

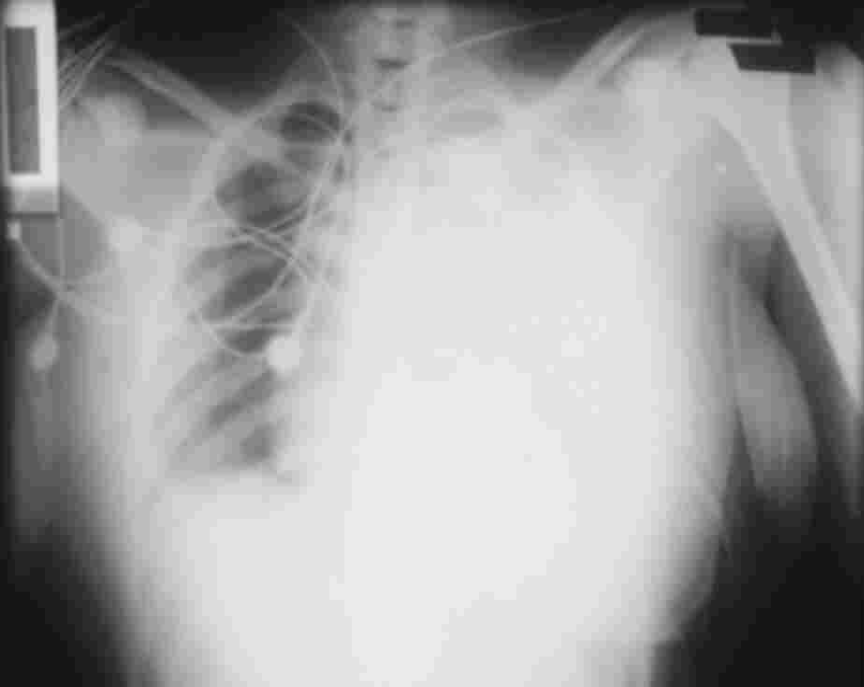


Nobel prizes

Roentgen (1901): Discovery of X-rays

Hounsfield & Cormack (1979): Computed tomography





Chest X-Ray

This frontal chest radiograph demonstrates a dense (radio-opaque) left lung field consistent with a hemothorax in a patient with a gunshot wound to the chest.



COMPUTED TOMOGRAPHY, CT

This CT image demonstrates the large bullae characteristic of patients with Chronic Obstructive Pulmonary Disease (**COPD**) representing lung destruction

CT DETECTORS

Detector Type

Xenon

Pressurised xenon gas



Ionisation



Electrical signal

Solid state

Ceramic or crystal scintillator



Photon capture



Light



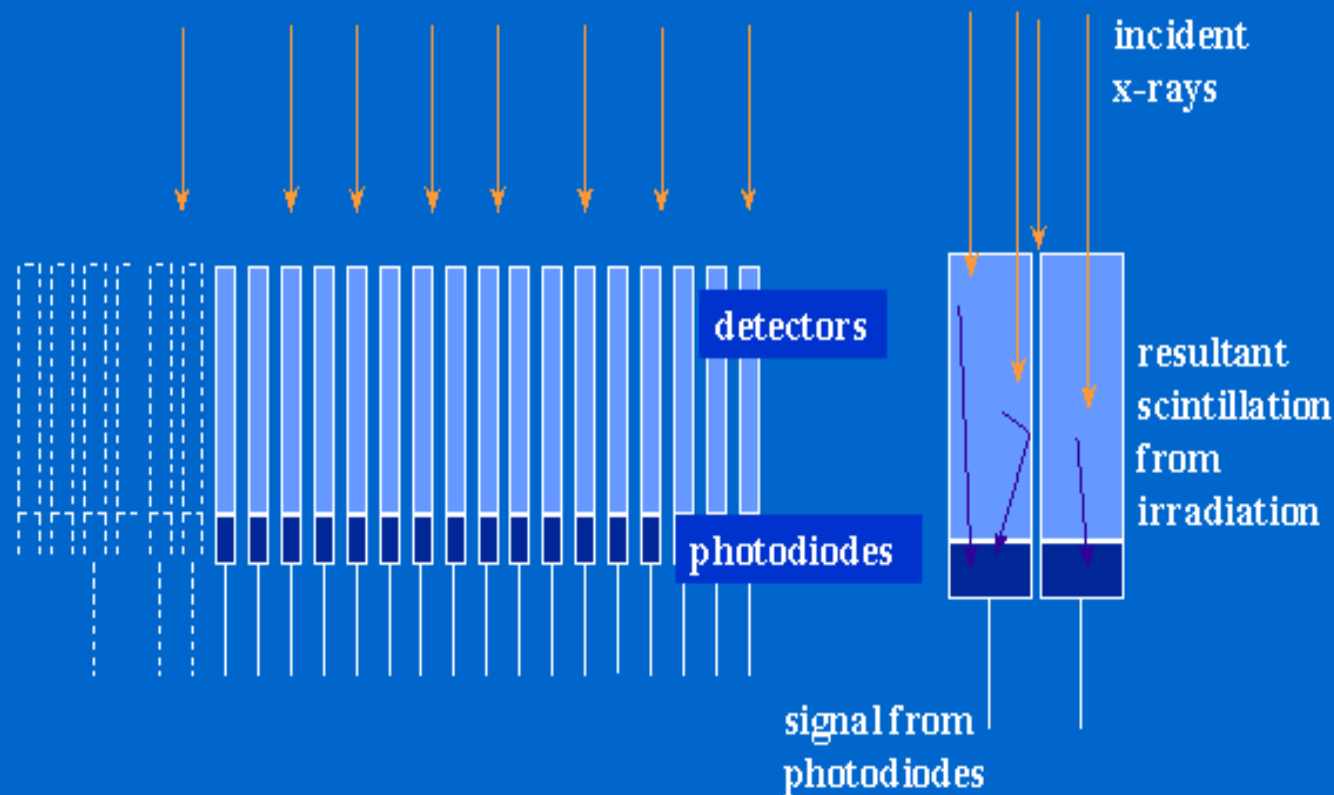
Photo-diode



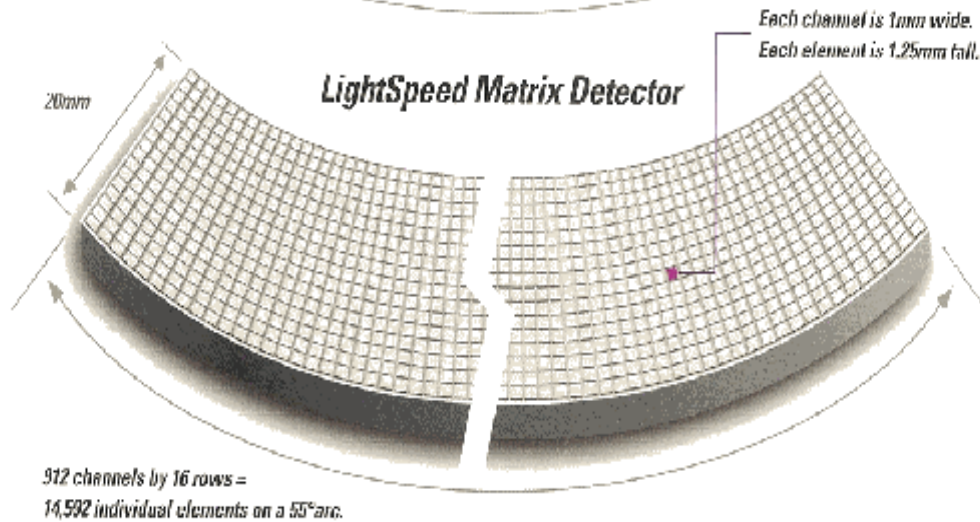
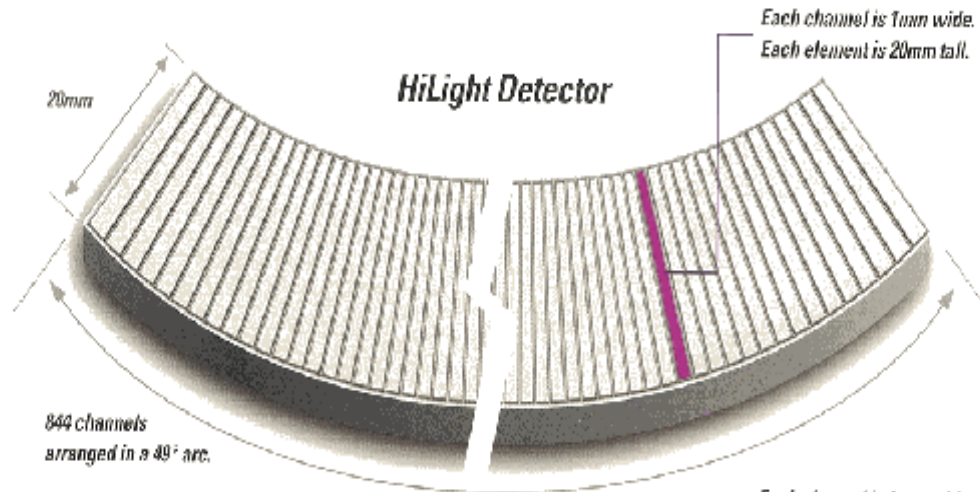
Electrical signal

CT DETECTORS

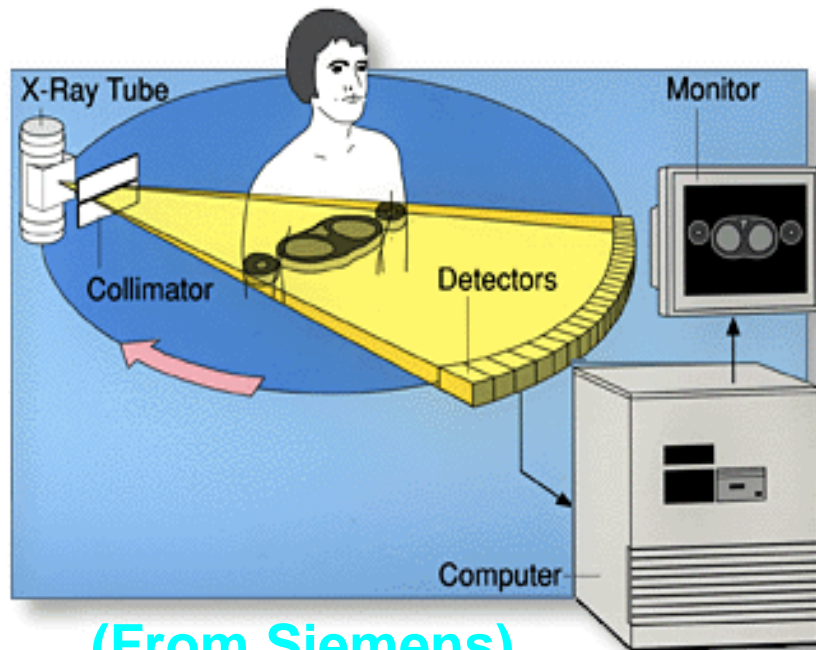
Solid State Detectors



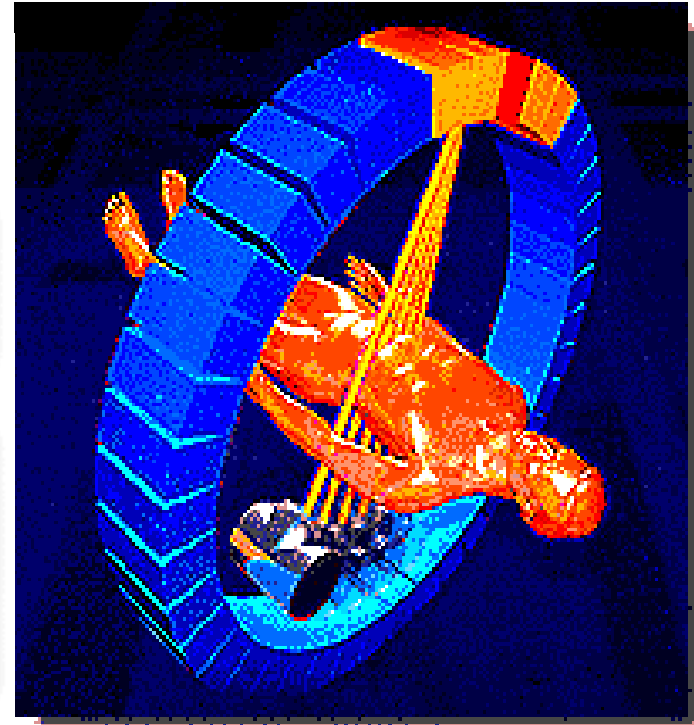
CT DETECTORS



Third & Fourth Generations



(From Siemens)

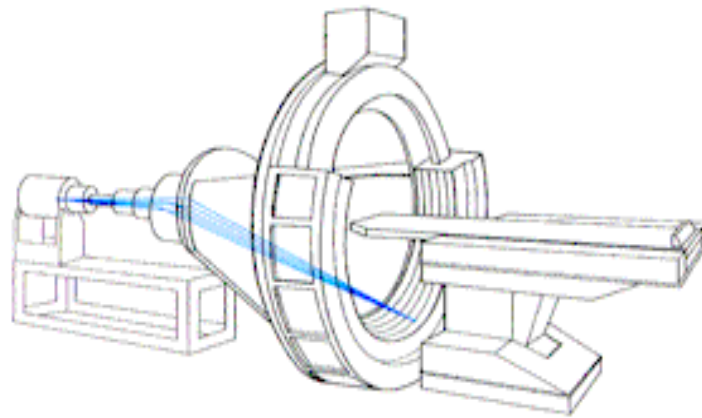


(From Picker)

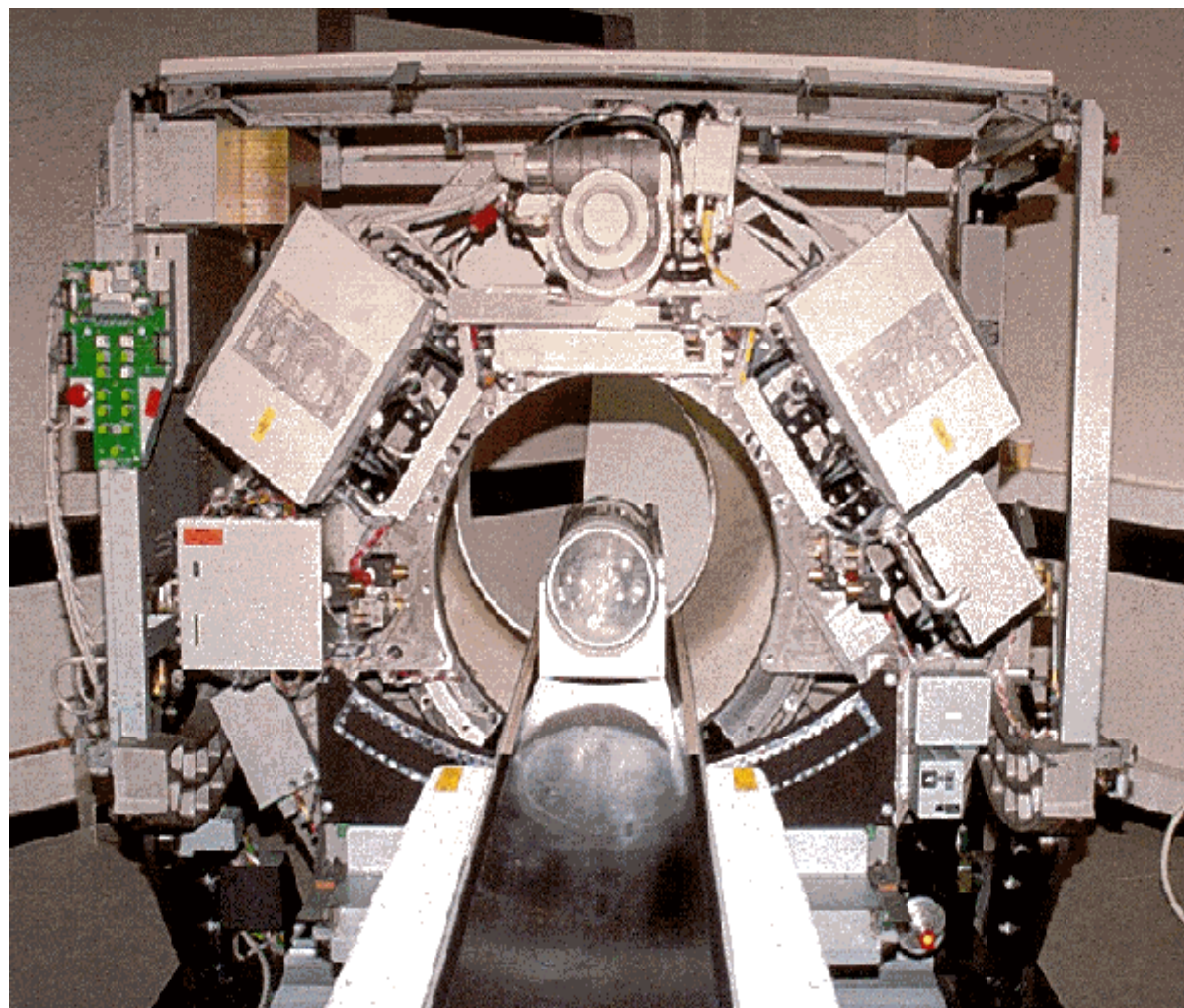
E-Beam CT Scanner

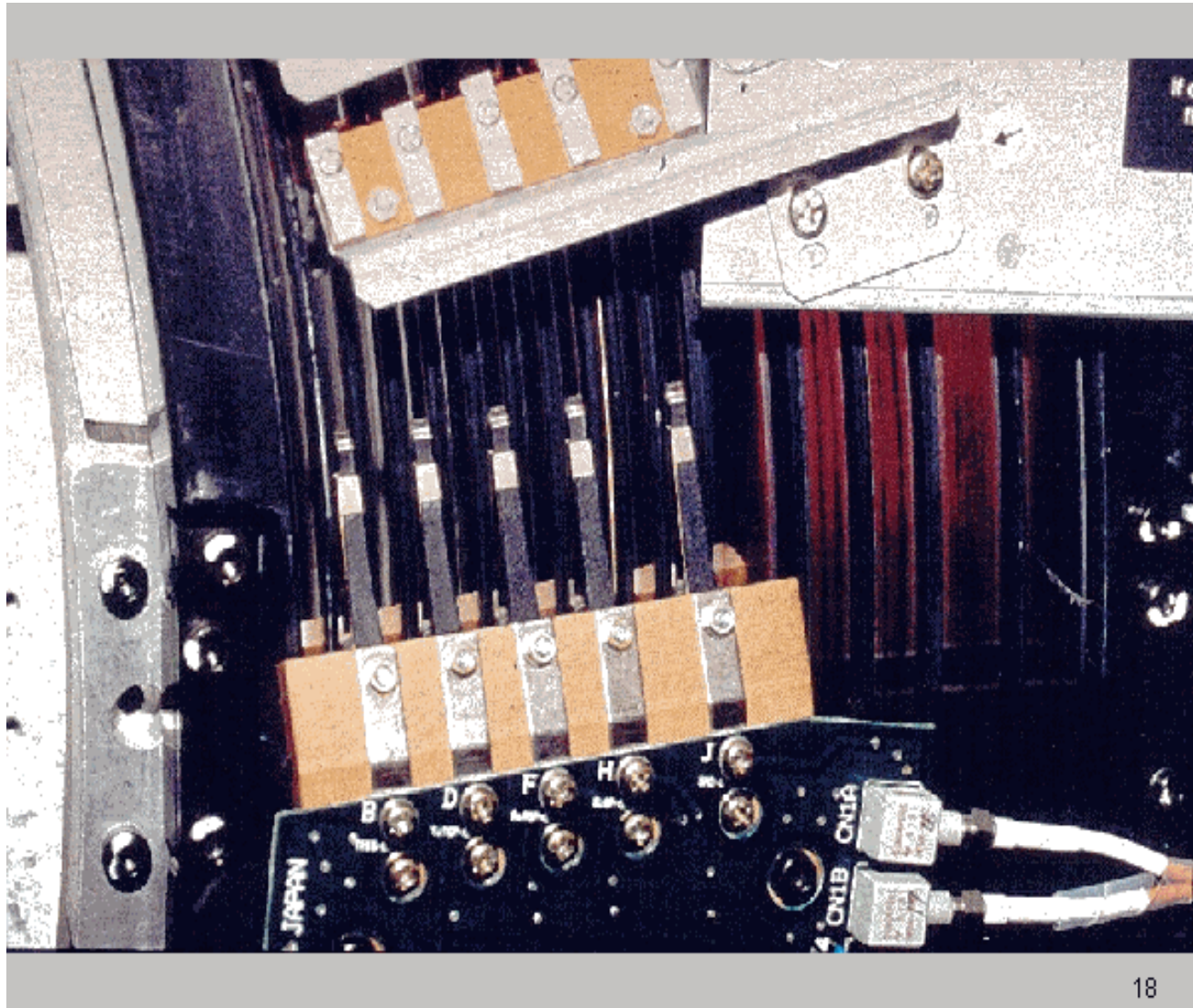


- Speed: 50, 100 ms
- Thickness: 1.5, 3, 6, 10 mm
- ECG trigger cardiac images



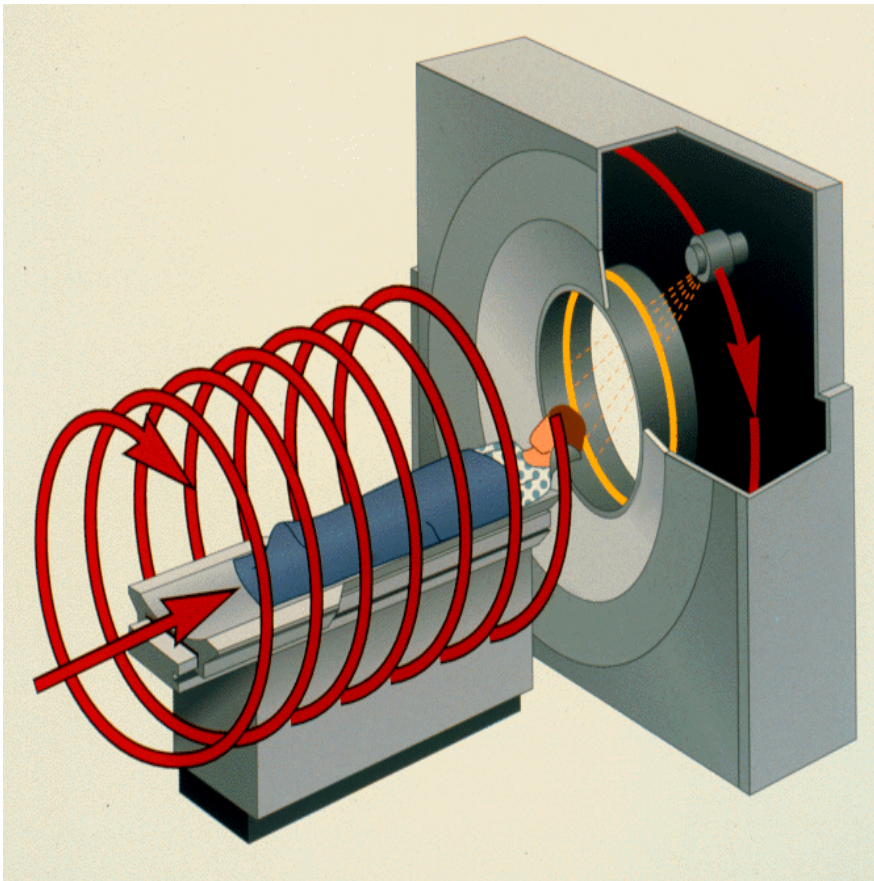
(From Imatron)







Spiral/Helical/Volumetric CT

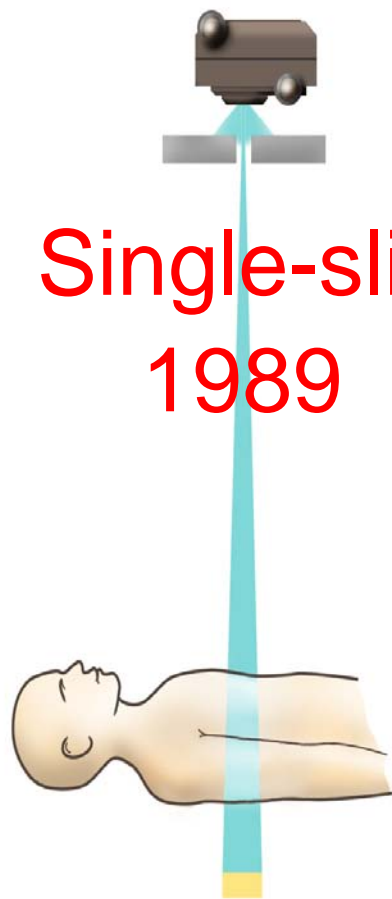


- Continuous &
Simultaneous**
- **Source rotation**
 - **Patient translation**
 - **Data acquisition**





A rapid development



Single-slice
1989



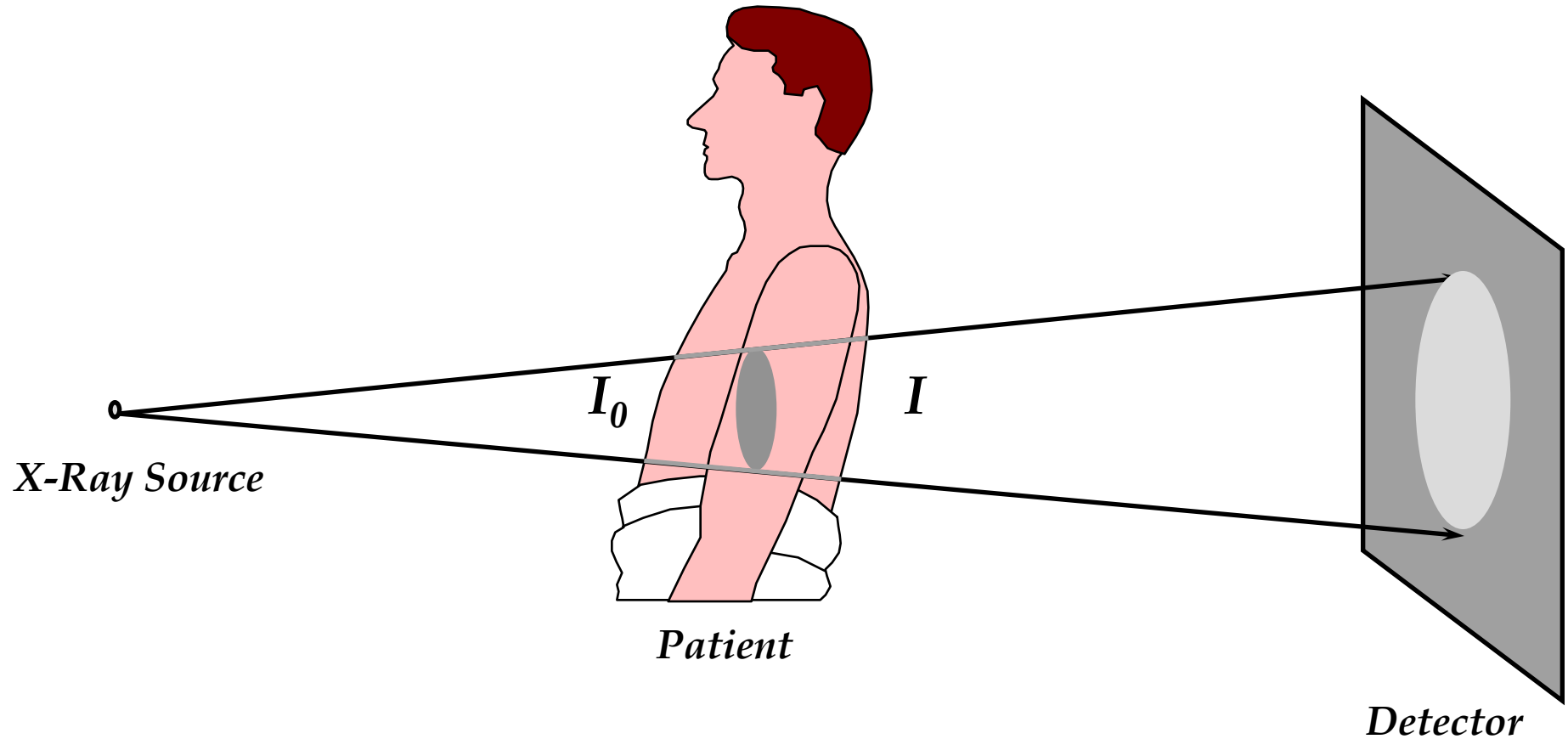
Dual-slice
1992



Quad-slice
1998



Projection Imaging with X Rays





Capabilities of slip-ring scanners (2)

- Cine scanning
(no table feed)
 - continuous series of images at one position
- “CT fluoroscopy”
 - new image reconstructed several times during one rotation





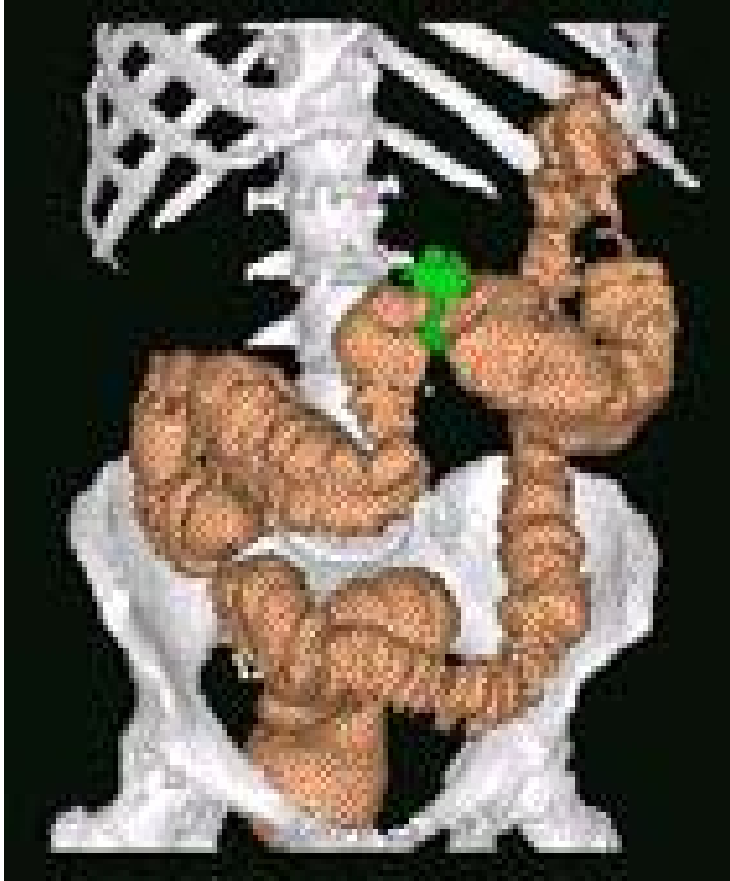
Capabilities of slip-ring scanners (3)

- Spiral scanning
(continuous table feed)
 - Image reconstruction at
 - any position
 - any interval } can choose retrospectively
 - Large volume can be scanned in a single breath hold





Image Analysis



Visualization & analysis

- 3D, 4D
 - Networked, PC-based
 - Image fusion
 - Computer aided diagnosis
 - Image-based surgery
- 



FUTURE

- **MONOENERGETIC RADIATION**
- **DUAL ENERGY AROUND THE K-EDGE**
- **ENERGY SENSITIVE PIXELDETECTORS**





IMAGE RECONSTRUCTION



Radon Transform

$$Rf(\vec{\theta}, s) = \int_{\Gamma} f(\vec{x}) dm(\vec{x})$$

$$\Gamma = [\vec{x} \in R^n : \langle \vec{x}, \vec{\theta} \rangle = s]$$

$$f(\vec{x}) \in C^{\infty}$$

Rapidly decreasing

Radon Operator R is defined in Schwartz spaces

$$S(R^n) \rightarrow S(Z^n) = S(S^{n-1} \times R)$$

Radon & Fourier Transforms

Fourier Transform

$$\tilde{f}(\vec{\xi}) = \int_{\mathbb{R}^n} f(\vec{x}) e^{-i\langle \vec{x}, \vec{\xi} \rangle} d\vec{x}$$

Fourier Slice Theorem

$$\tilde{f}(\alpha\vec{\theta}) = \int_{-\infty}^{\infty} Rf(\vec{\theta}, s) e^{-i\alpha s} ds, \alpha \in \mathbb{R}$$

Backprojection

Dual Operator

$$R^{\#} g(\vec{x}) = \int_{S^{n-1}} g(\vec{\theta}, \langle \vec{x}, \vec{\theta} \rangle) d\vec{\theta}, g \in S(Z^n)$$

$$(R^{\#} g)^* f = R^{\#} (g^* Rf)$$

Derivative-Free Fan-Beam Formula

$$g(x, y) = \frac{1}{2} \int_0^{2\pi} \frac{\rho^2(\beta)}{(\rho(\beta) - s)^2} \int_{-\infty}^{\infty} R(p, \beta) f\left(\frac{\rho(\beta)t}{\rho(\beta) - s} - p\right) \frac{\rho(\beta)}{\sqrt{\rho^2(\beta) + p^2}} dp d\beta$$

$$t = x \cos \beta + y \sin \beta$$

$$s = -x \sin \beta + y \cos \beta$$

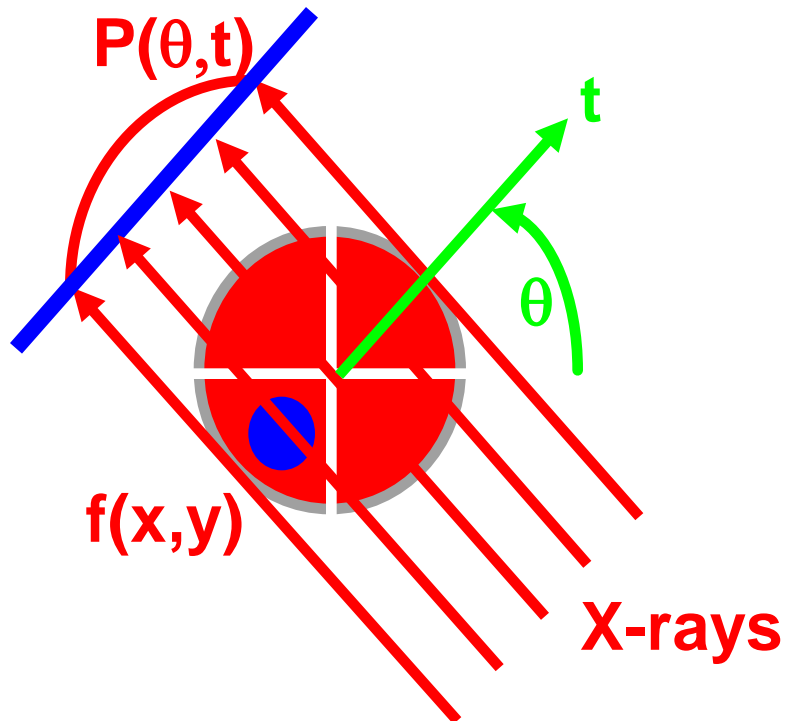
$$\rho(\beta) = \sqrt{t^2 + s^2}$$

- $\rho(\beta) = \rho(\beta + \pi)$
- $\rho'(\beta)$ exists almost everywhere
- Jacobi > 0

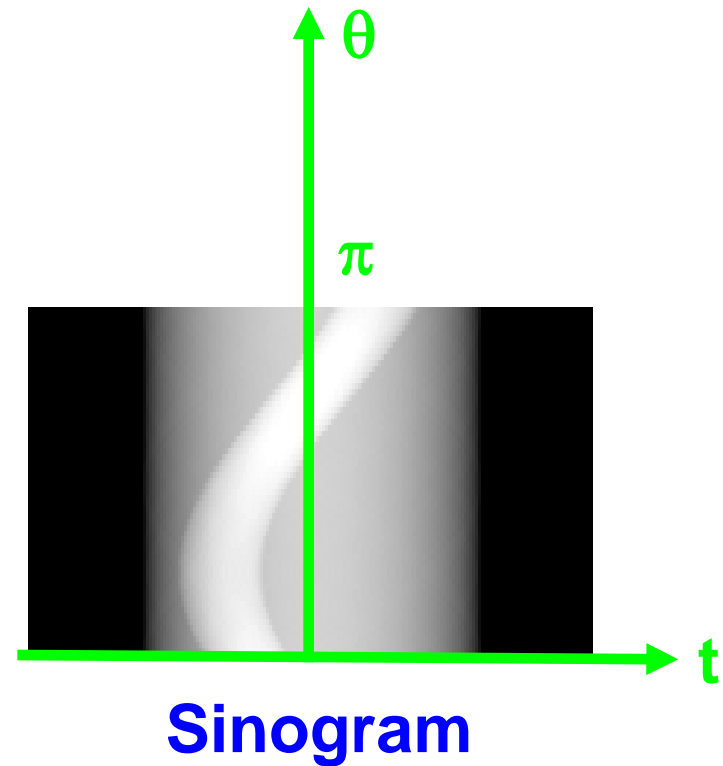
Wang, Lin, Cheng: IEEE TIP 2:543-547, 1993

Projection & Sinogram

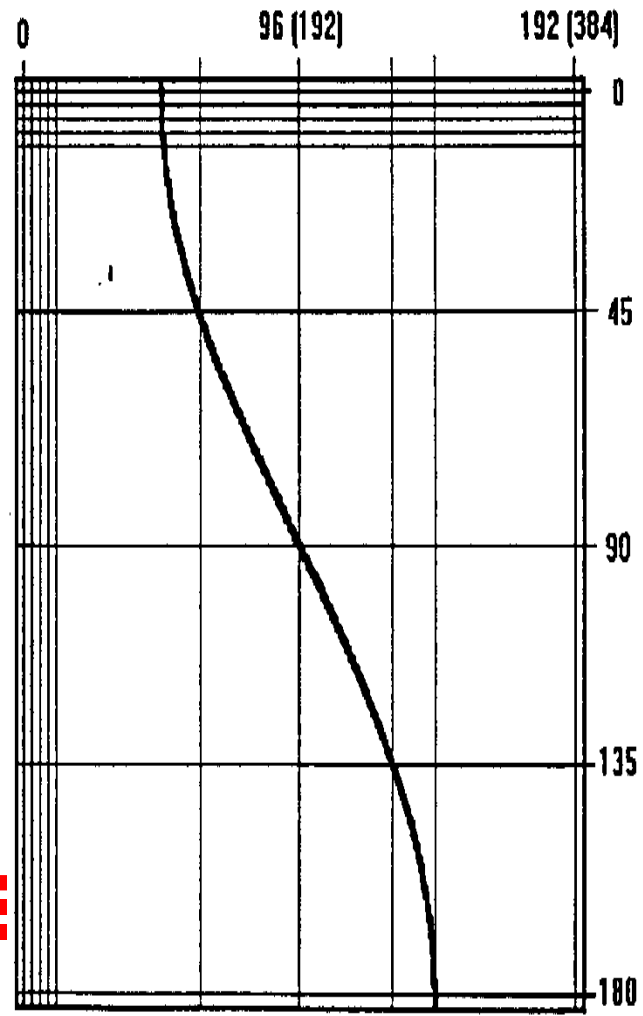
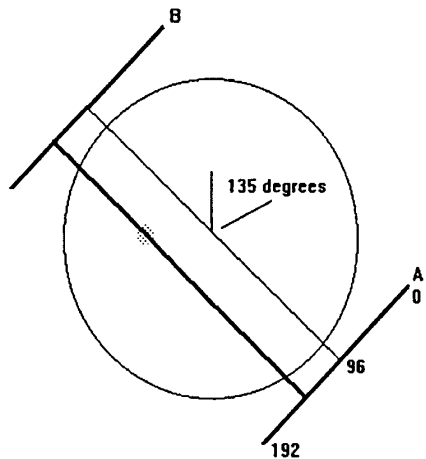
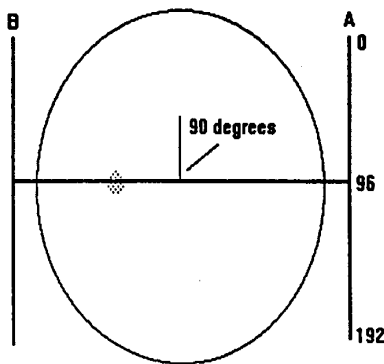
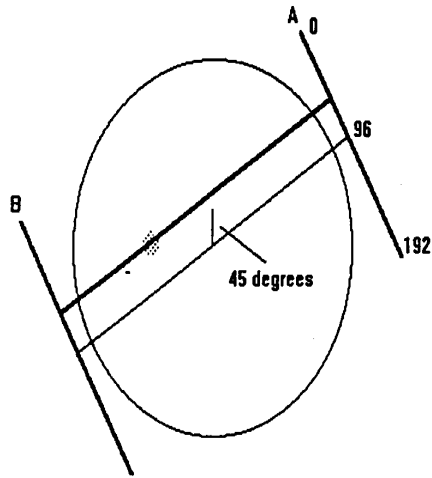
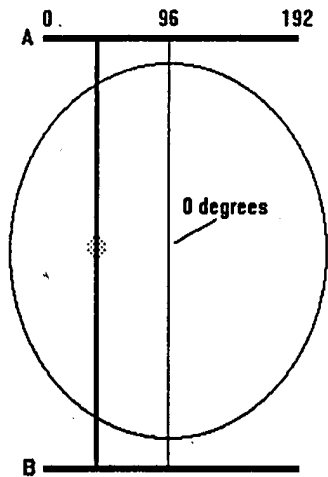
Projection:
All ray-sums in a direction



Sinogram:
All projections



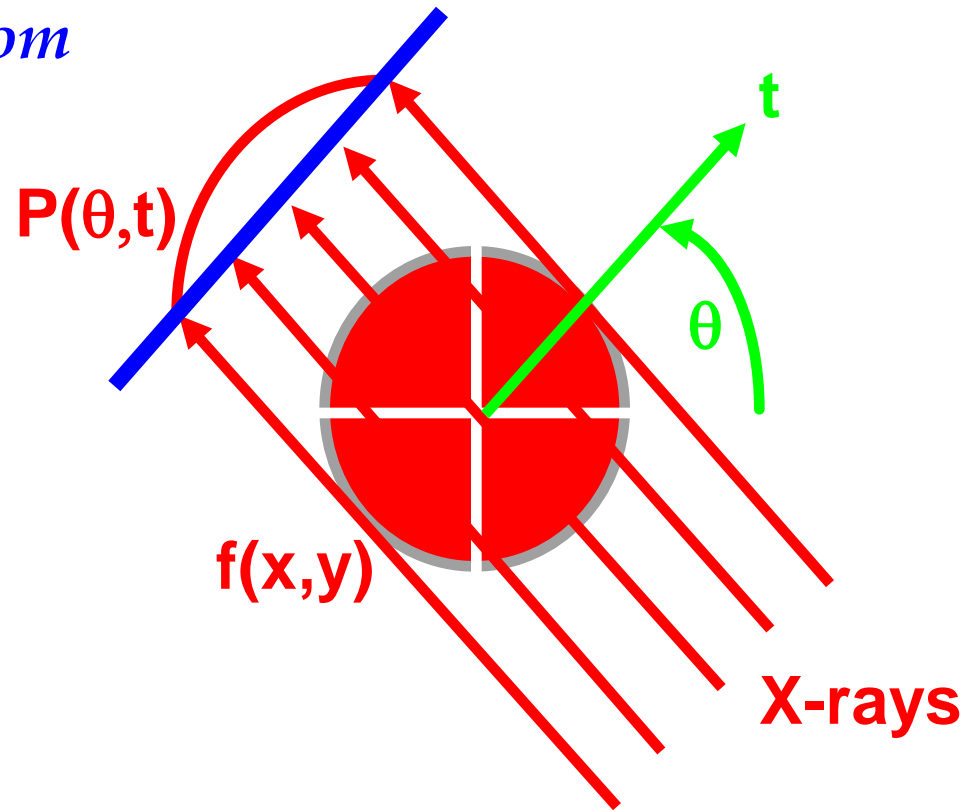
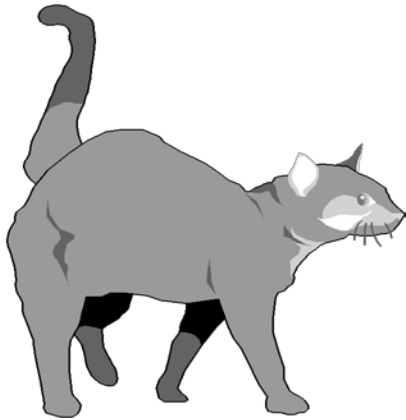
SINOGRAM CONSTRUCTION



Computed Tomography

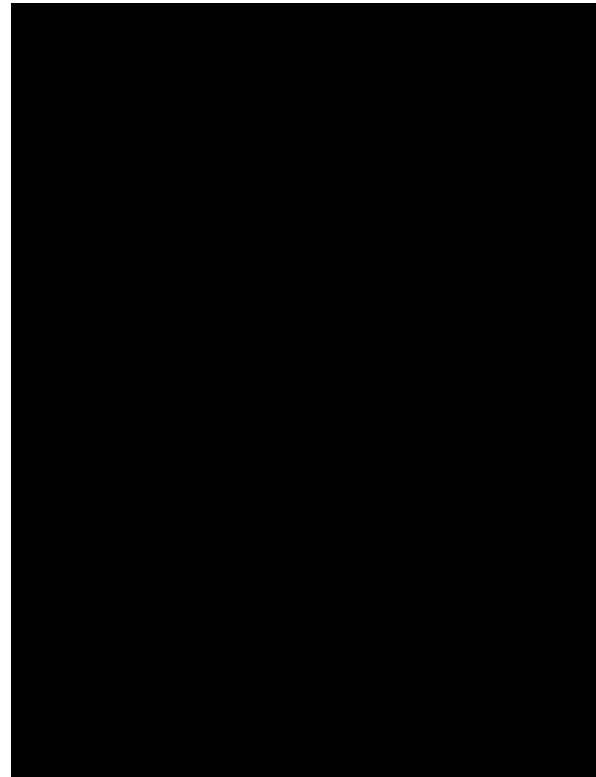
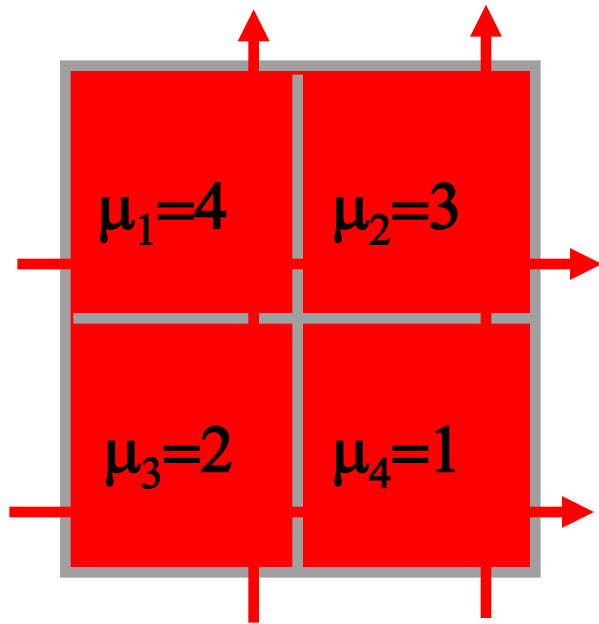
Computed tomography (CT):
Image reconstruction from
projections

$P(\theta, t) \Rightarrow f(x, y)$

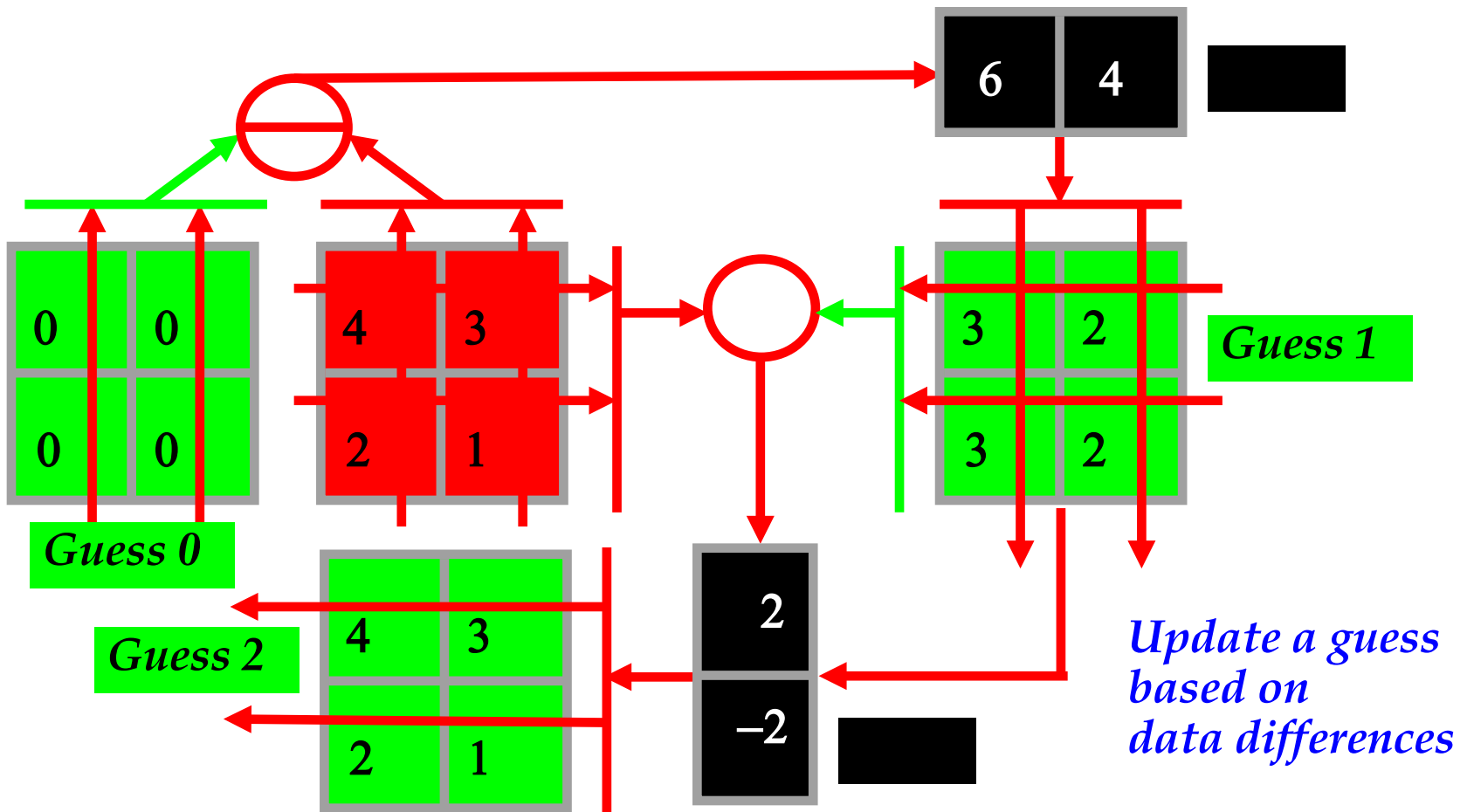




Reconstruction Idea

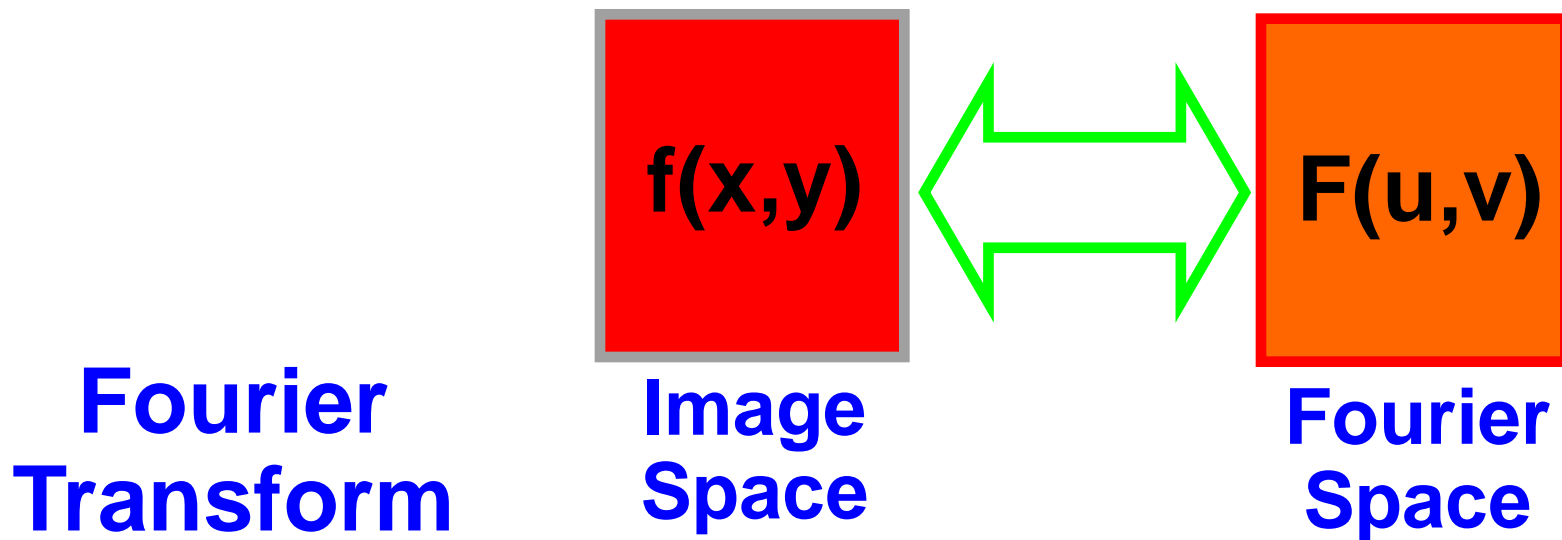


Algebraic Reconstruction Technique (ART)






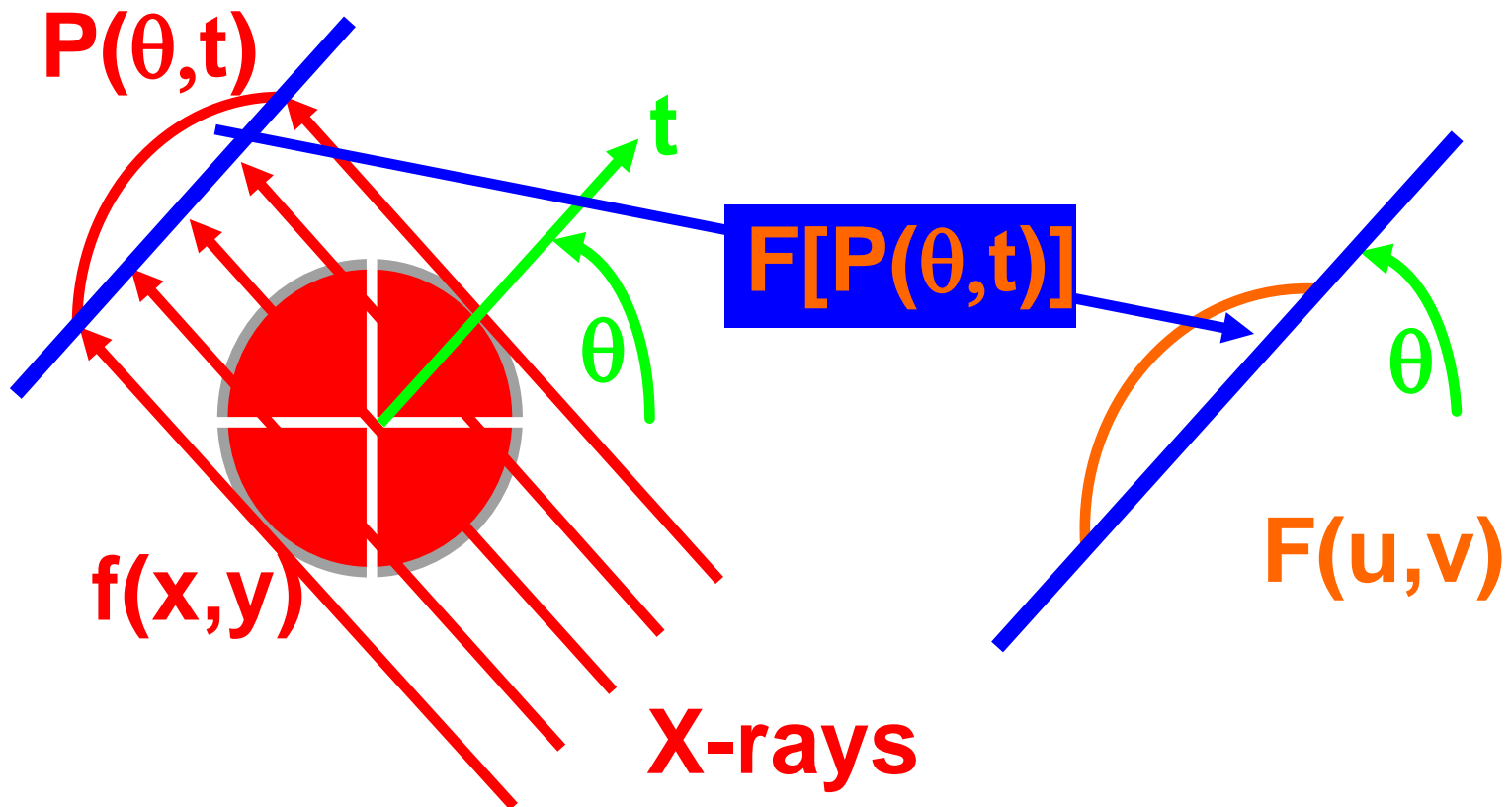
Fourier Transformation



$$F(u, v) = F[f(x, y)] = \int_{-\infty}^{\infty} \int_{-\infty}^{\infty} f(x, y) e^{-j2\pi(ux+vy)} dx dy$$

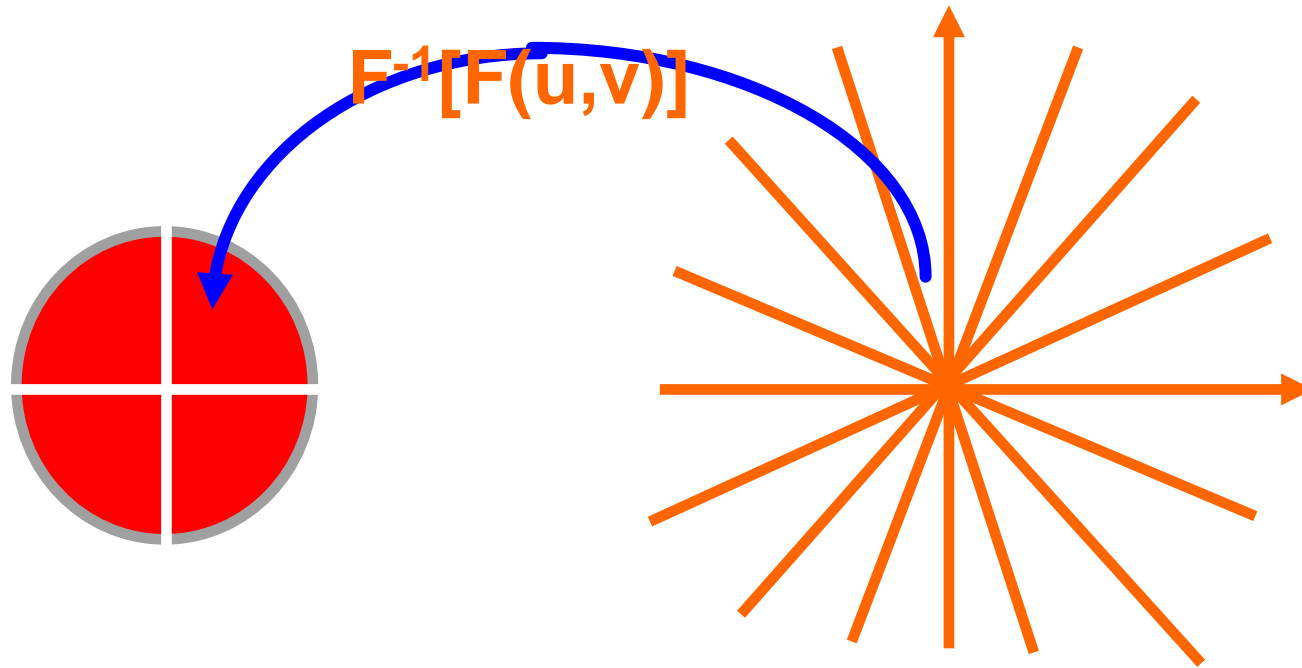
$$f(x, y) = F^{-1}[F(u, v)] = \int_{-\infty}^{\infty} \int_{-\infty}^{\infty} F(u, v) e^{j2\pi(ux+vy)} du dv$$


Fourier Slice Theorem

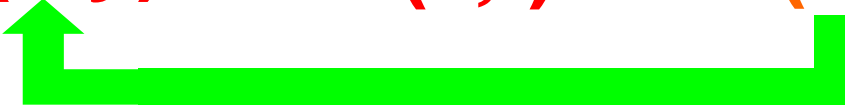




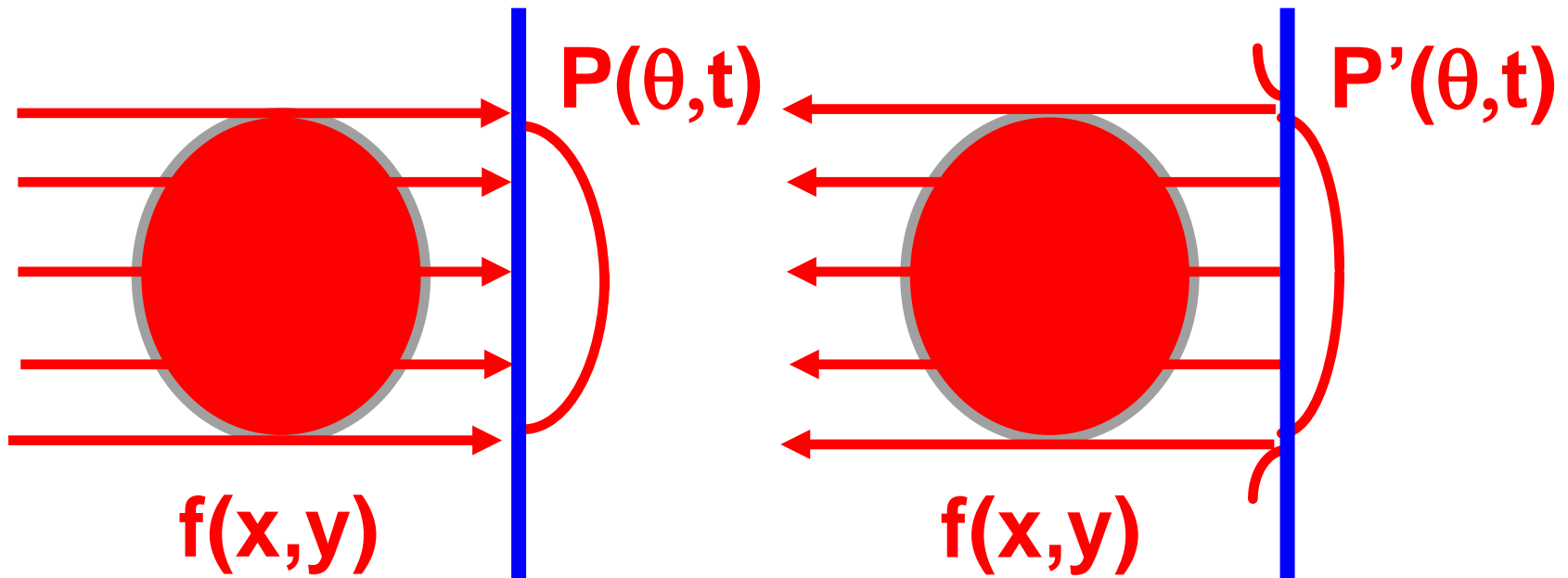
From Projections to Image



$f(x,y) \rightarrow P(\theta,t) \rightarrow F(u,v)$



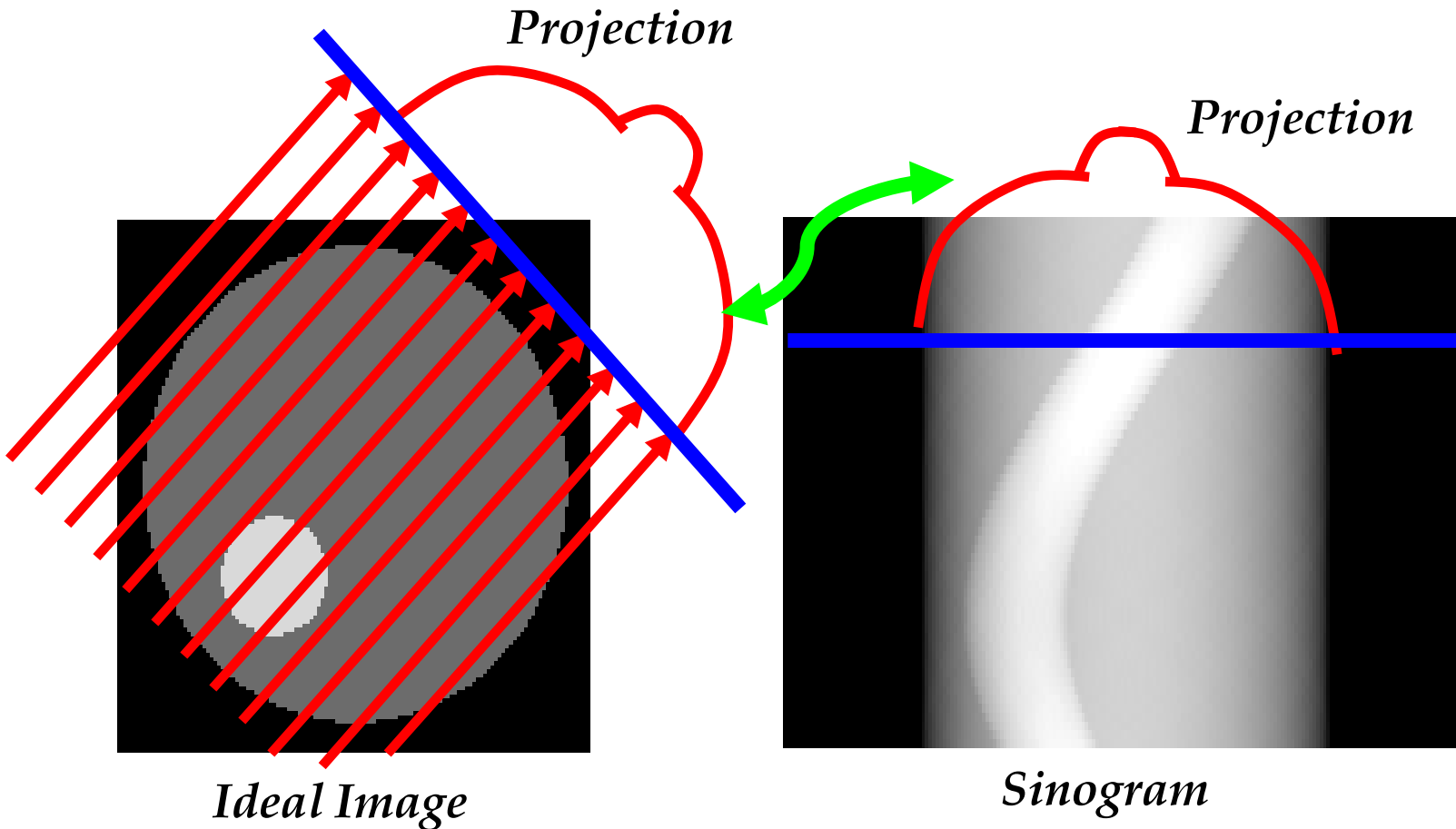
Filtered Backprojection



- 1) Convolve projections with a filter
- 2) Backproject filtered projections

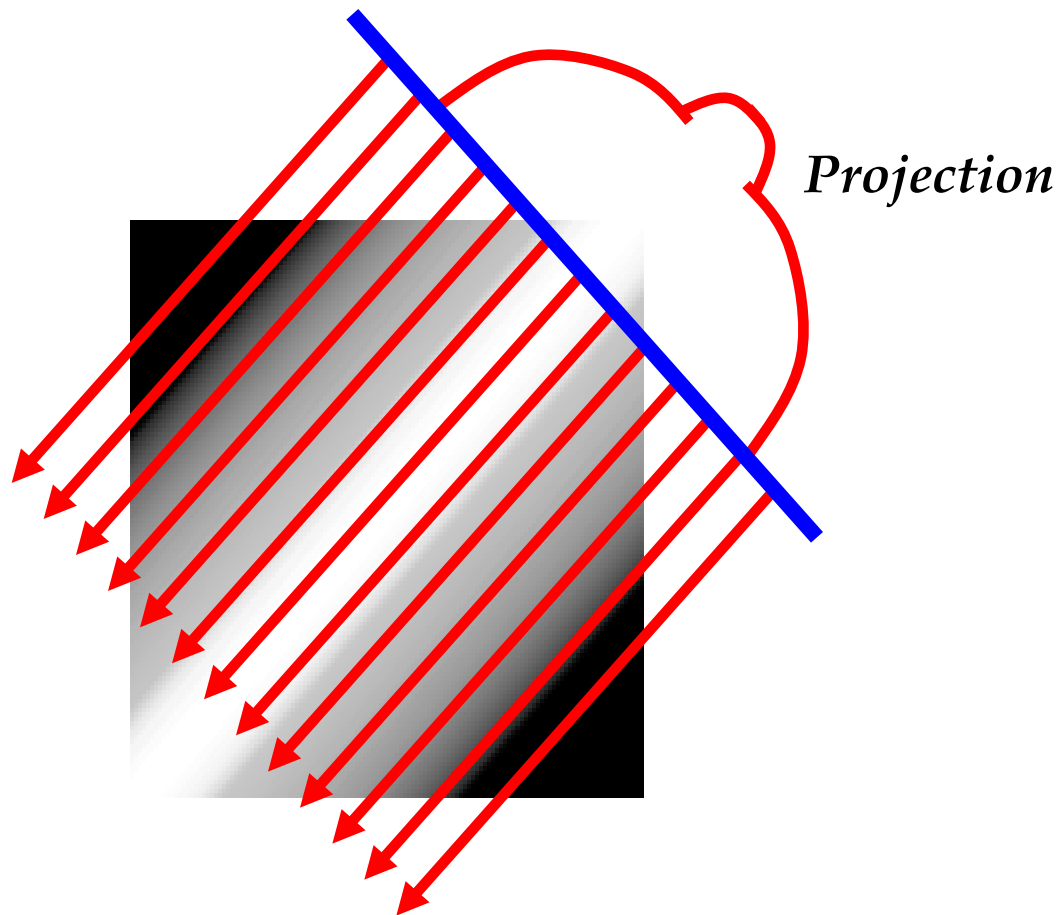


Example: Projection





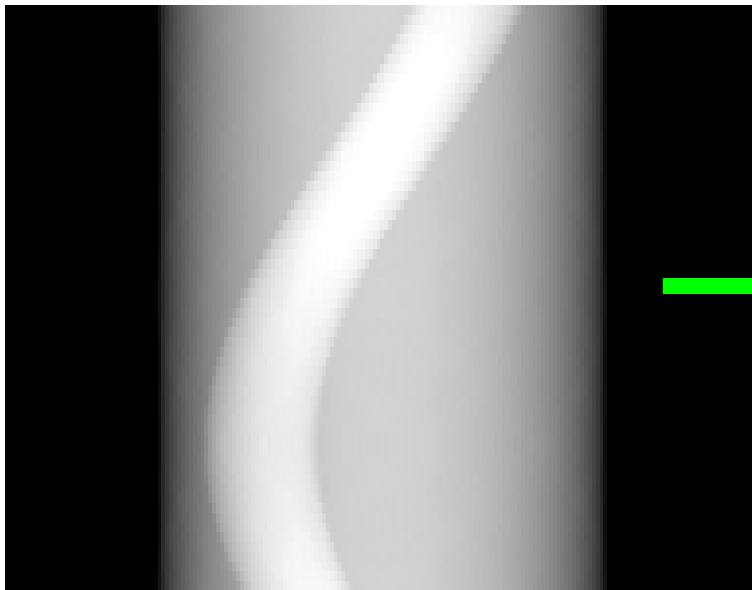
Example: Backprojection



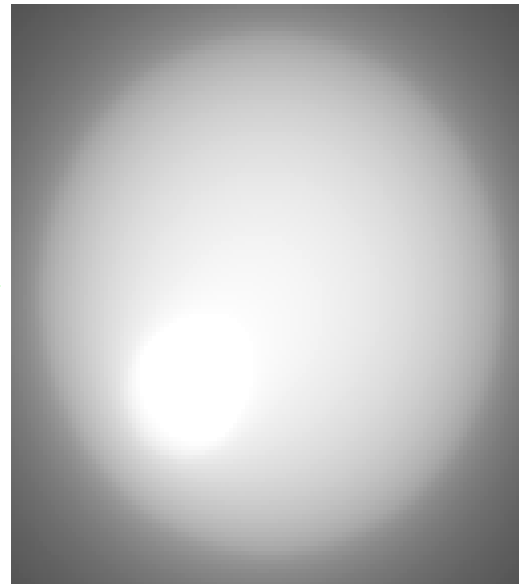


Example: Backprojection

Sinogram



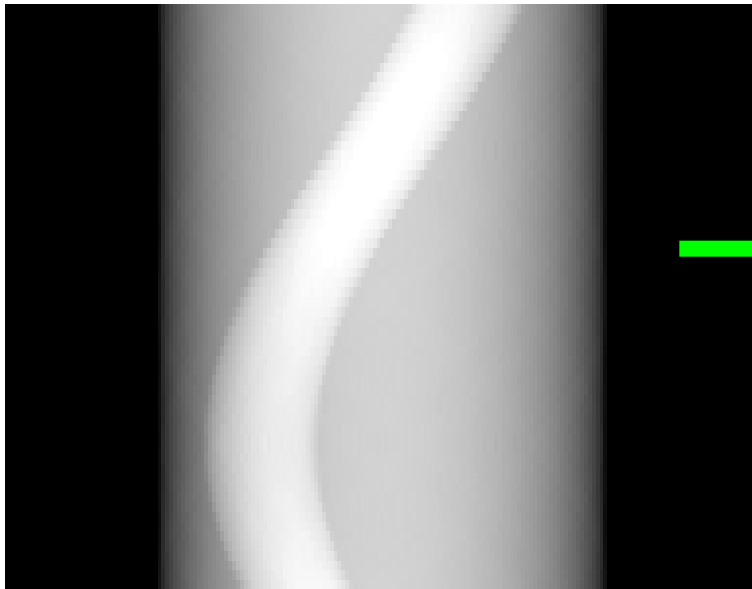
Backprojected Image



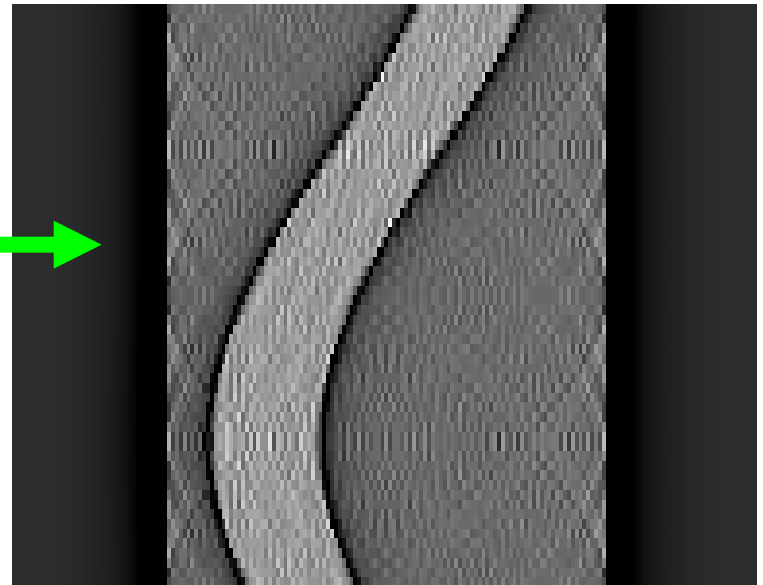


Example: Filtering

Sinogram



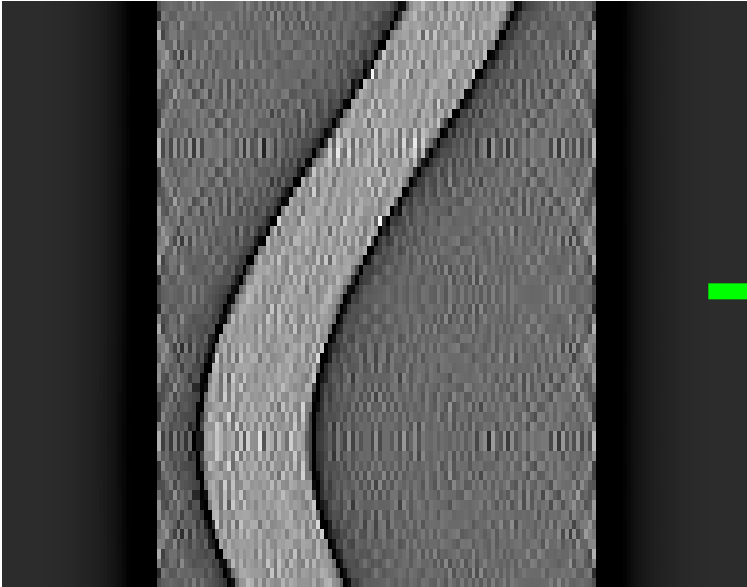
Filtered Sinogram



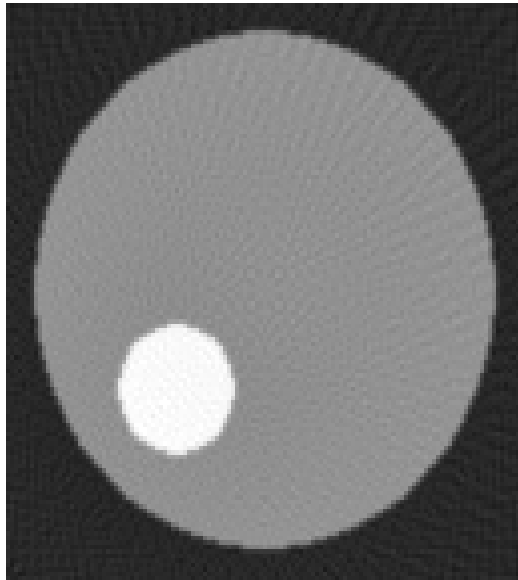


Example: Filtered Backprojection

Filtered Sinogram



Reconstructed Image



Some examples



Linefbkp.mov



Brainbkp.mov



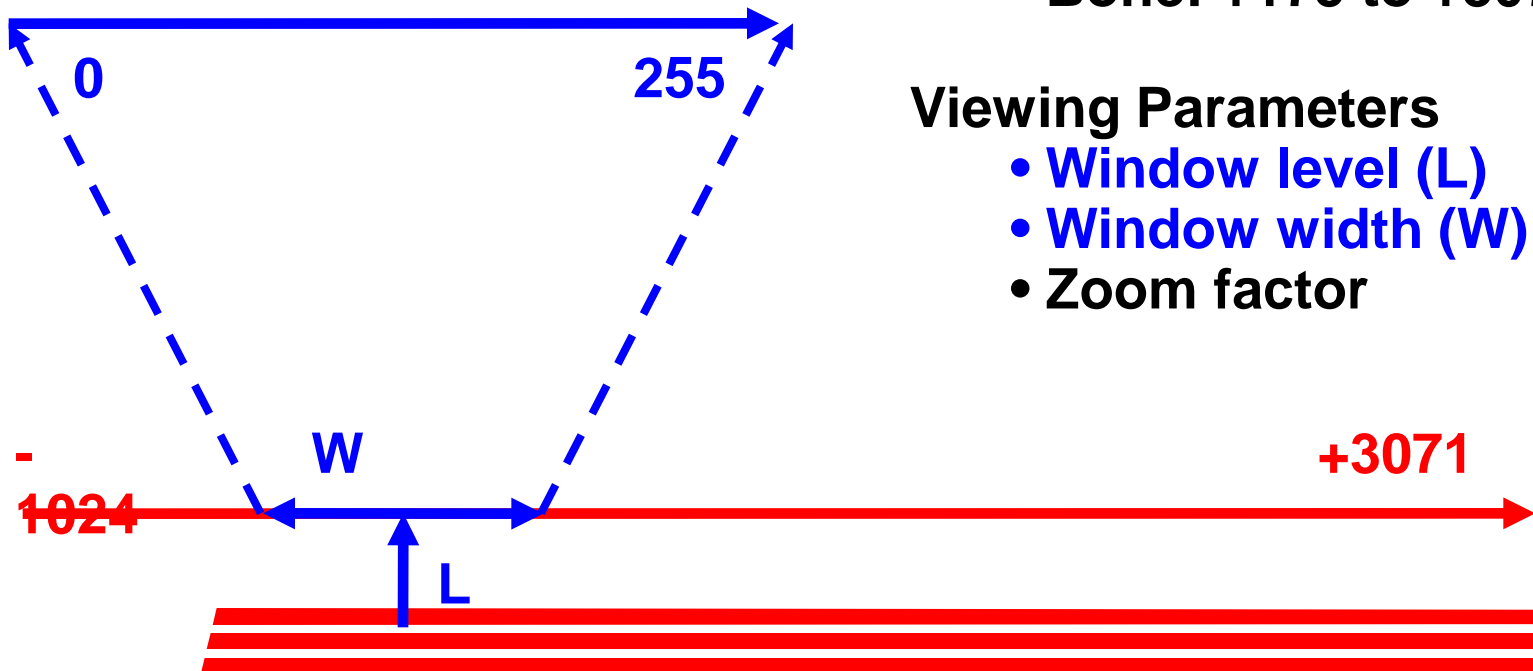
brainfbkp.mov



Skull.mov

Image Display

$$HU(\mu) = 1000 \frac{\mu - \mu_{water}}{\mu_{water}}$$



CT Number

- Hounsfield unit

- Air: -1024
- Water: 0
- Bone: +175 to +3071

Viewing Parameters

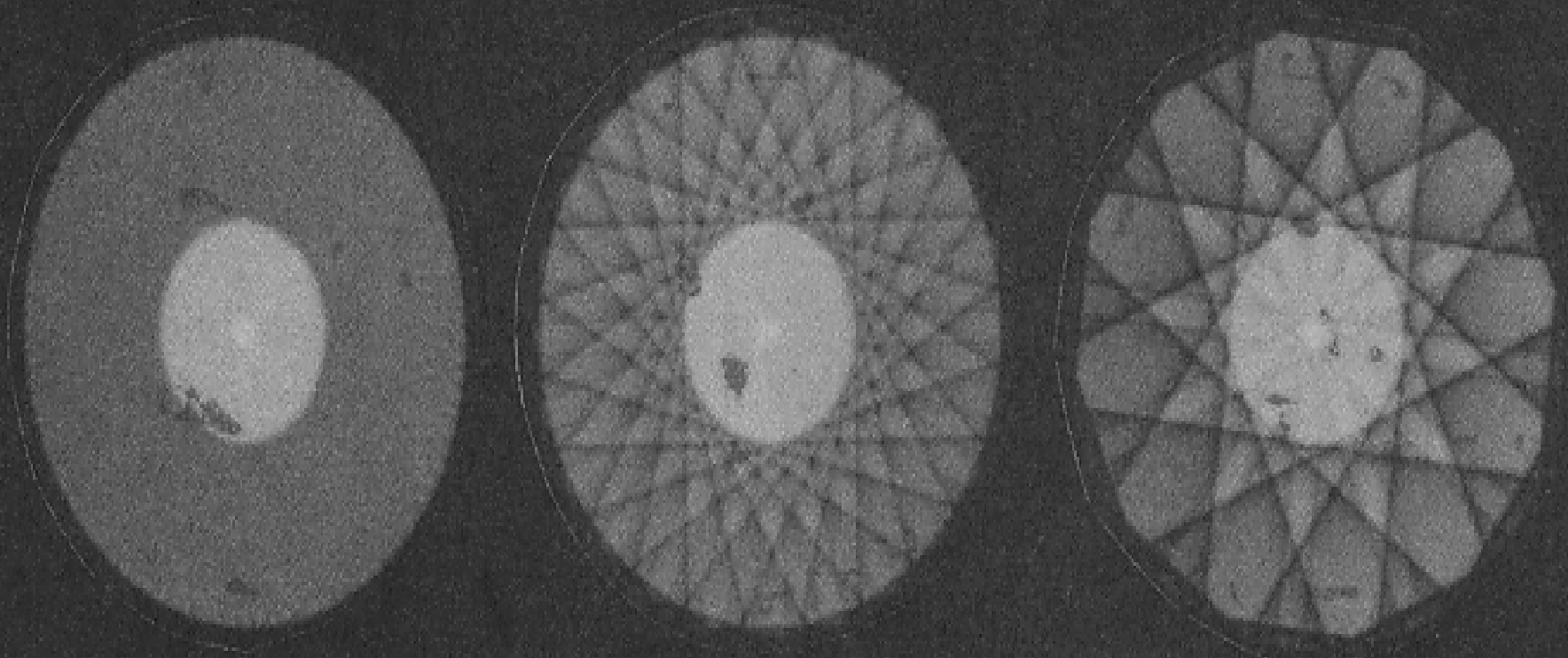
- Window level (L)
- Window width (W)
- Zoom factor



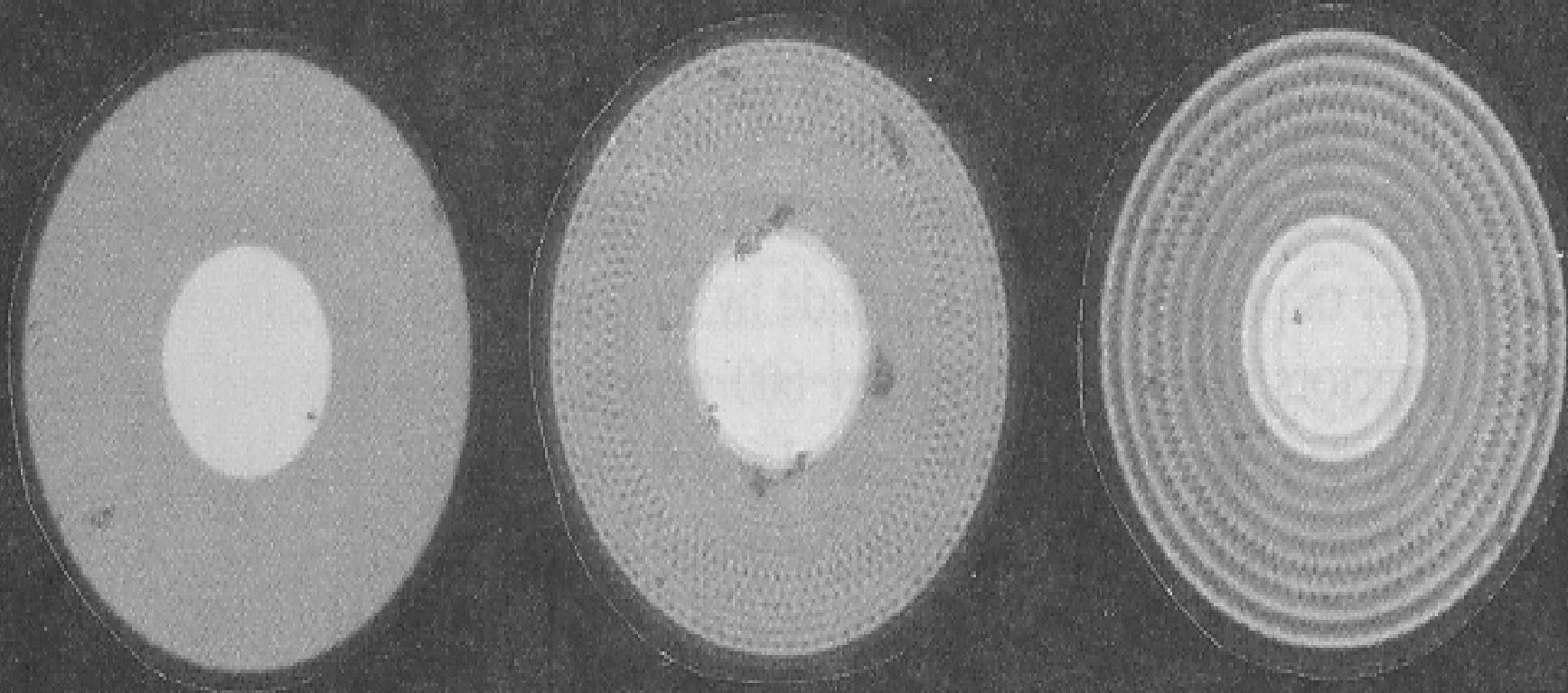
ARTIFACTS



Different numbers of projections (96, 24, 12)
Each projection contains 200 rays



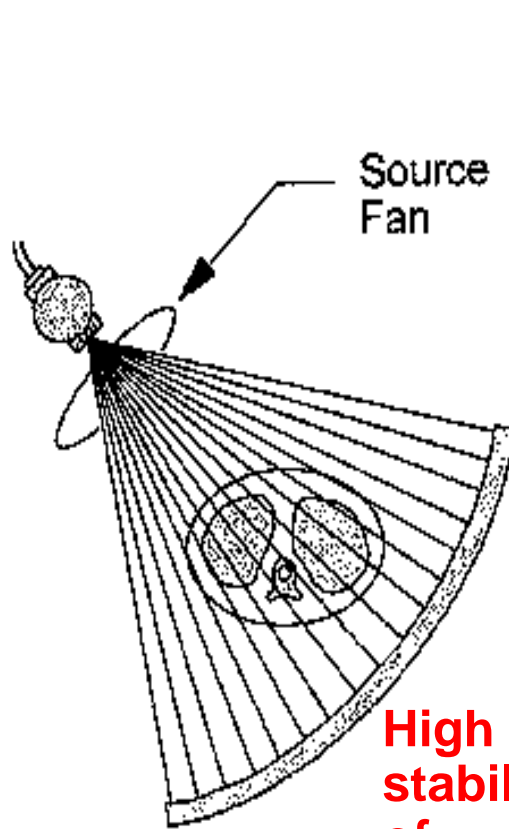
Number of projections (100). The projections have varying numbers of rays (200, 50, 25)



Comparison 3rd and 4th generation

3rd generation has the X-ray tube in the apex (source fan)

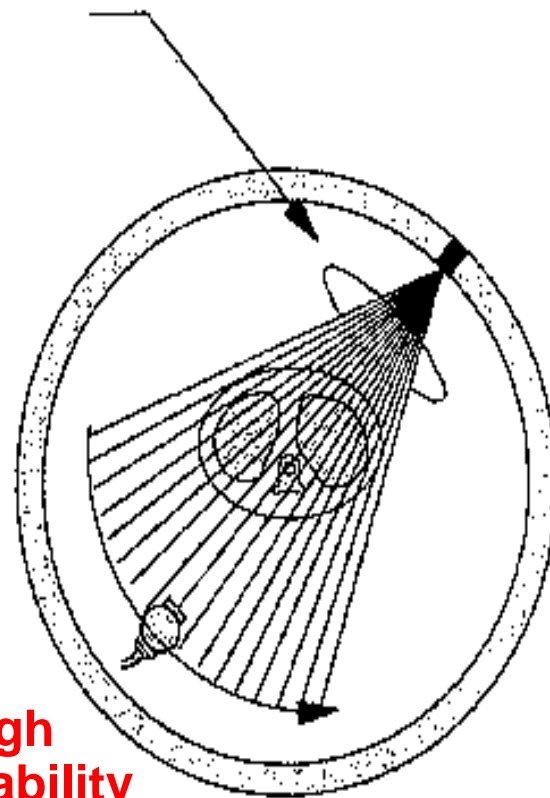
4th generation has a single detector in apex (detector fan)



Third
Generation

High
stability
of
detectors

Detector
Fan



High
stability
output of
X-ray
tube

Fourth
Generation

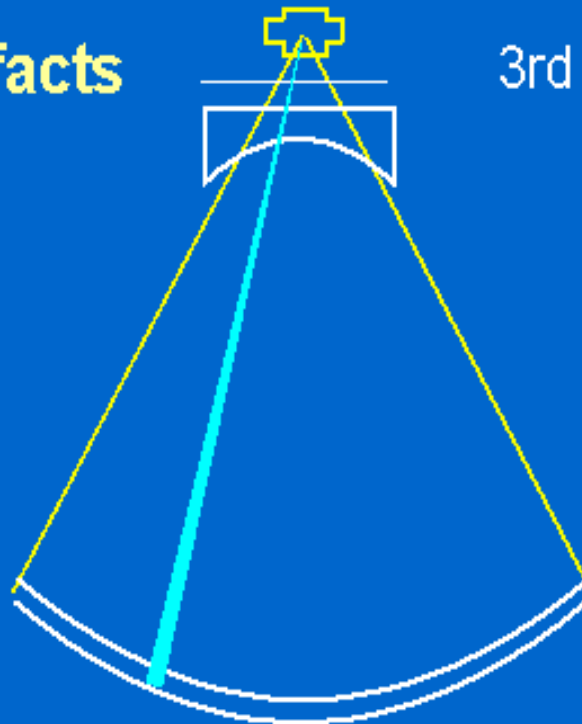


Problems with a bad detector is handled differently in 3rd and 4th generation

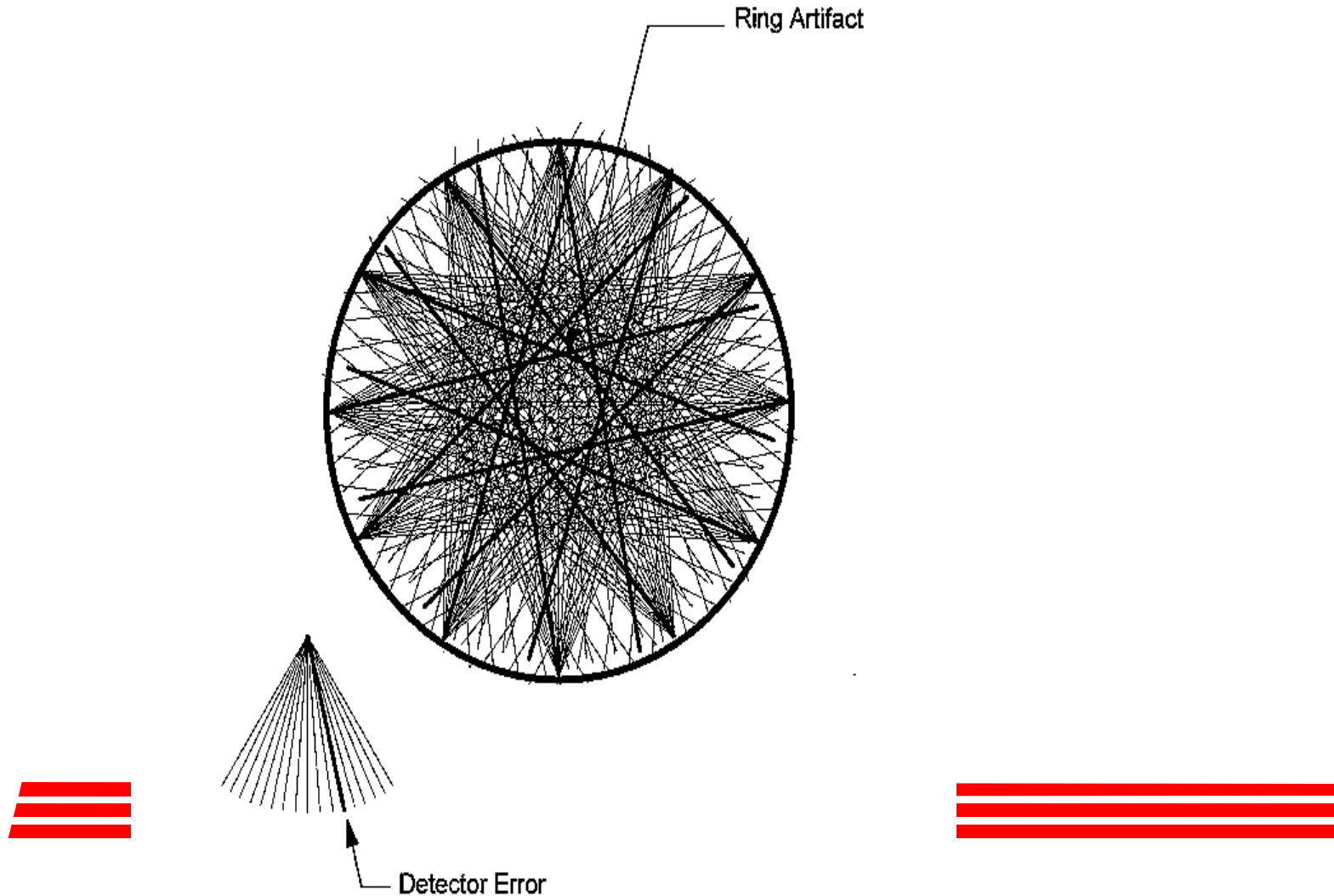
3rd generation v. 4th generation

Ring Artefacts

3rd generation



One detector that is bad in the 3rd generation will create a ring artifact. A small ring diameter if central and a large diameter for a peripheral detector.





Beam-Hardening Artifacts

Cause

Effective energy is shifted to higher value as the X-rays pass through an object

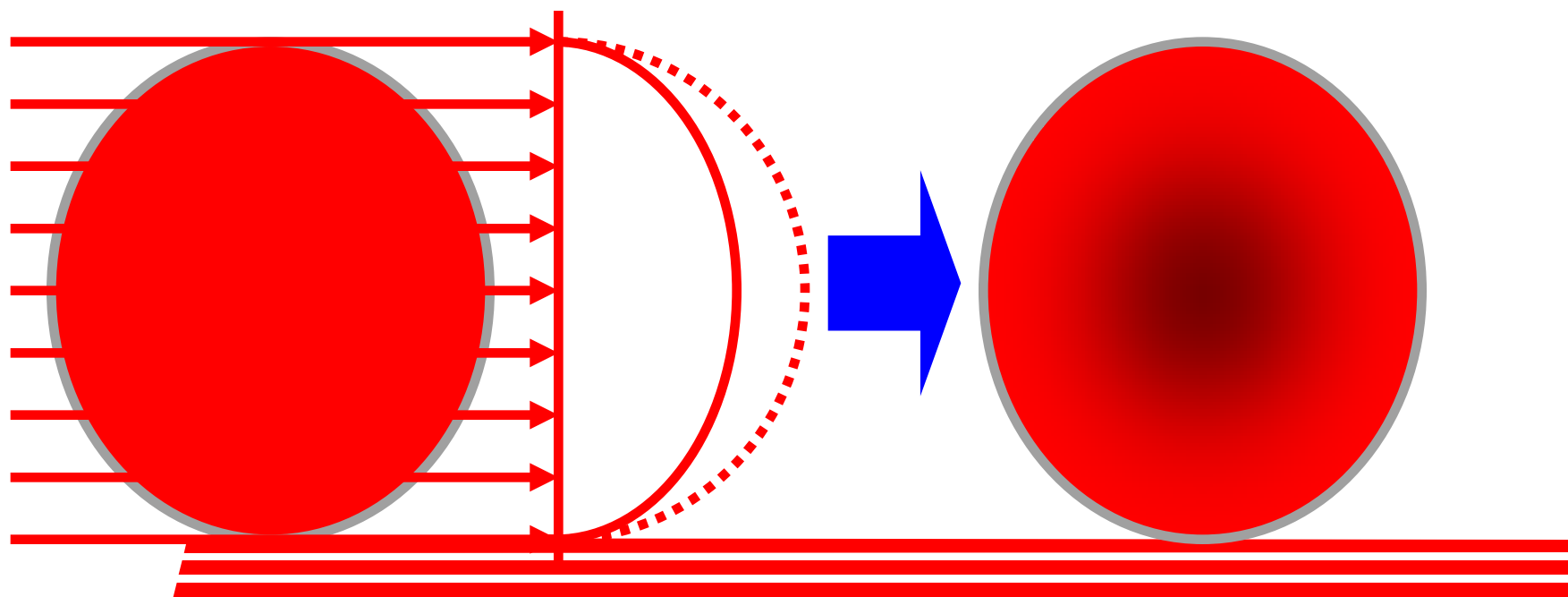
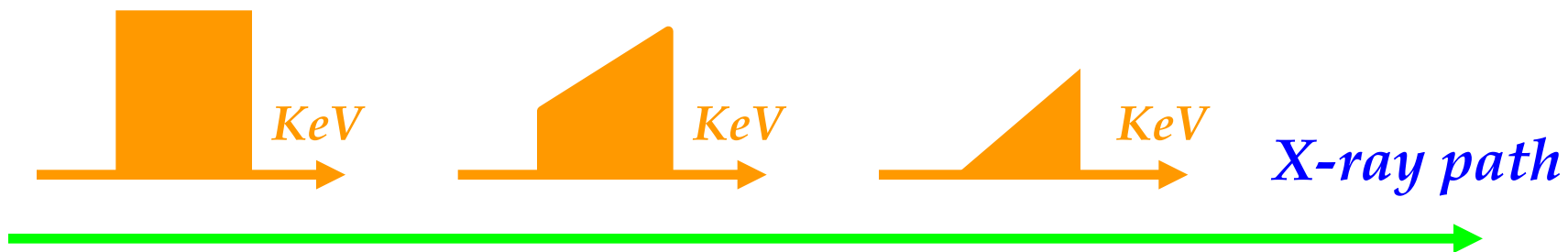
Correction

- **Pre-filter the X-ray beam near the focus**
- **Avoid highly absorbing bony regions**
- **Algorithms**





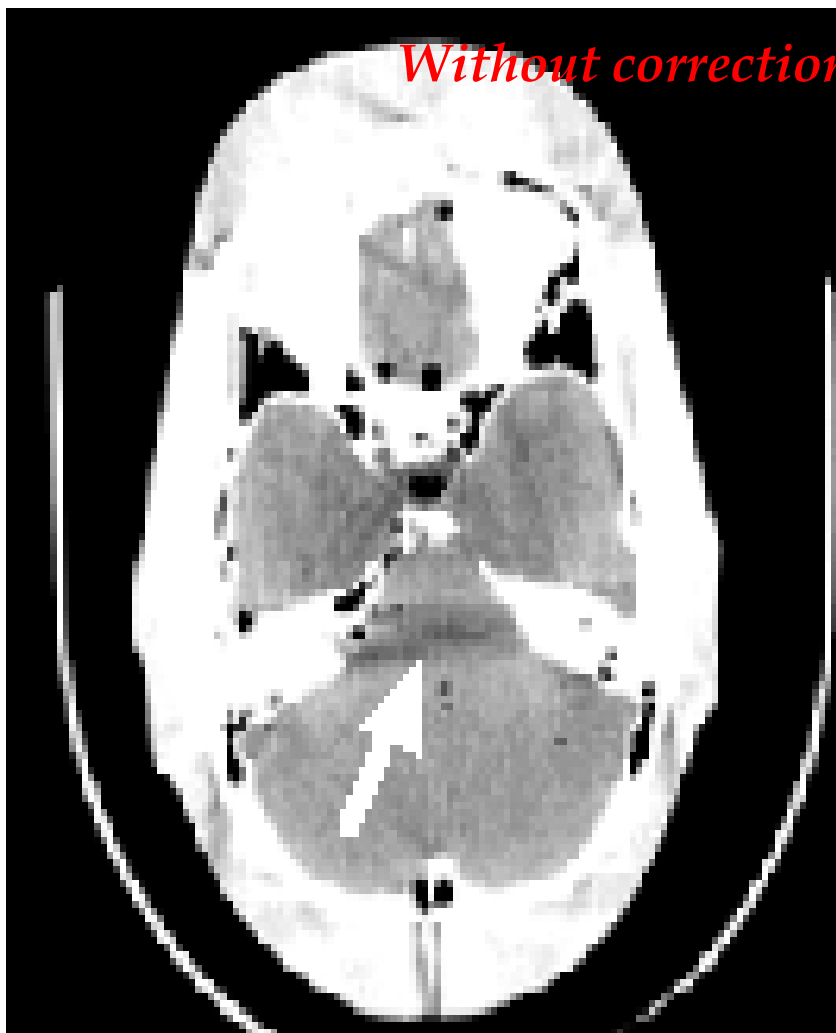
Beam-Hardening Artifacts





Beam-Hardening Artifacts (From J Hsieh at GE)

Without correction



With correction





Blurring Artifacts (Volume Averaging)

Causes

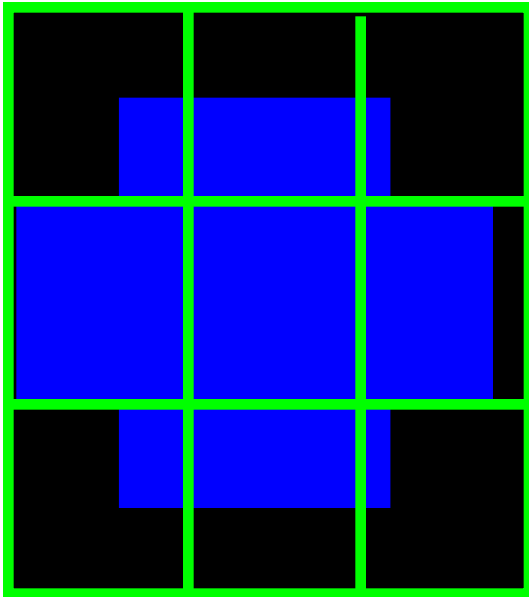
- **Large CT slice thickness and high contrast structures only partially included**
- **Finite source size**
- **Finite sampling rates**

Correction

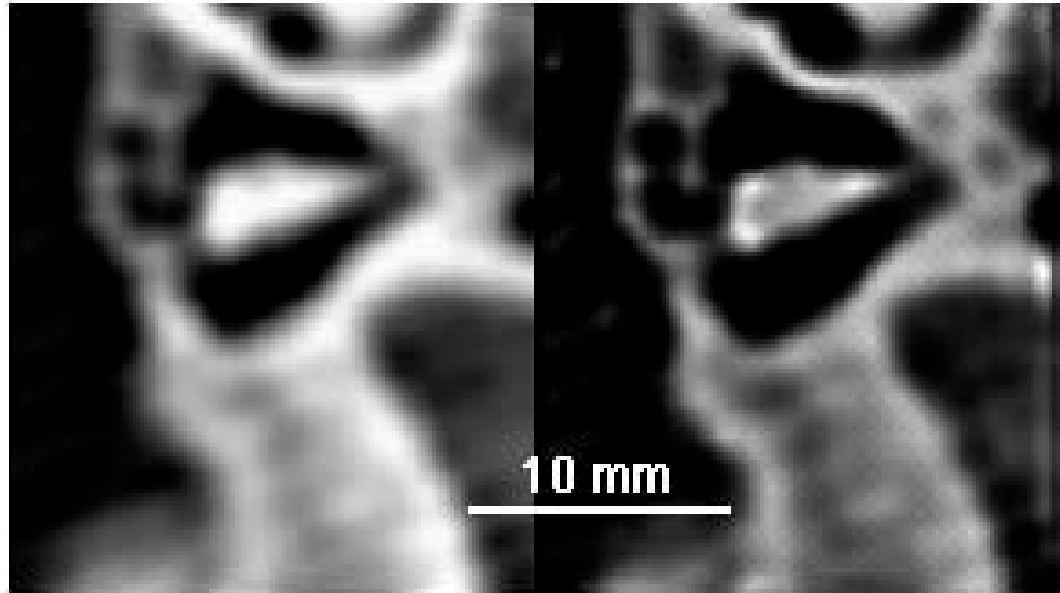
- **Volume Artifact Reduction (VAR) mode**
 - **Deblurring**
- 



Blurring Artifacts (Volume Averaging)



Volume averaging



Blurred

Deblurred

(Blurred data from GH Esselman at Wash U)





Stair-Step Artifacts (Helix)

Associated with inclined surfaces in reformatted slices

Causes

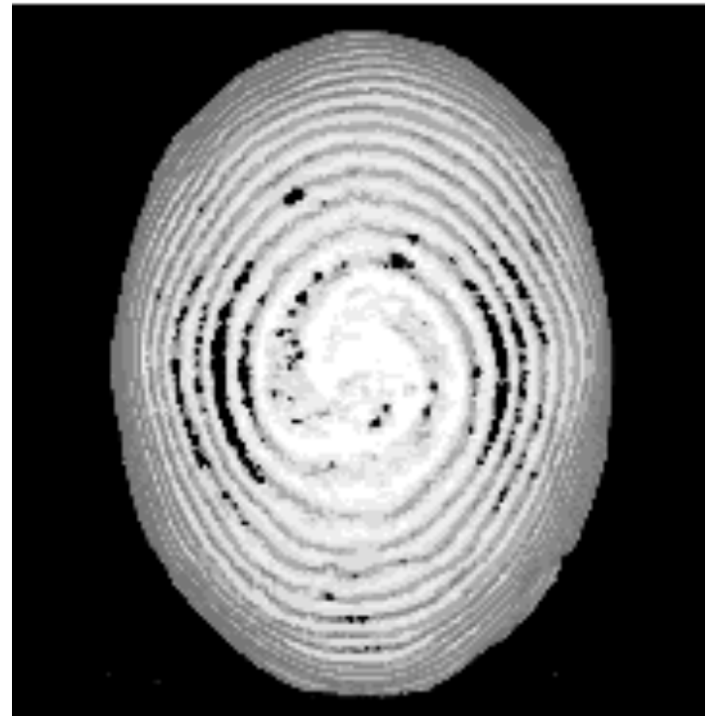
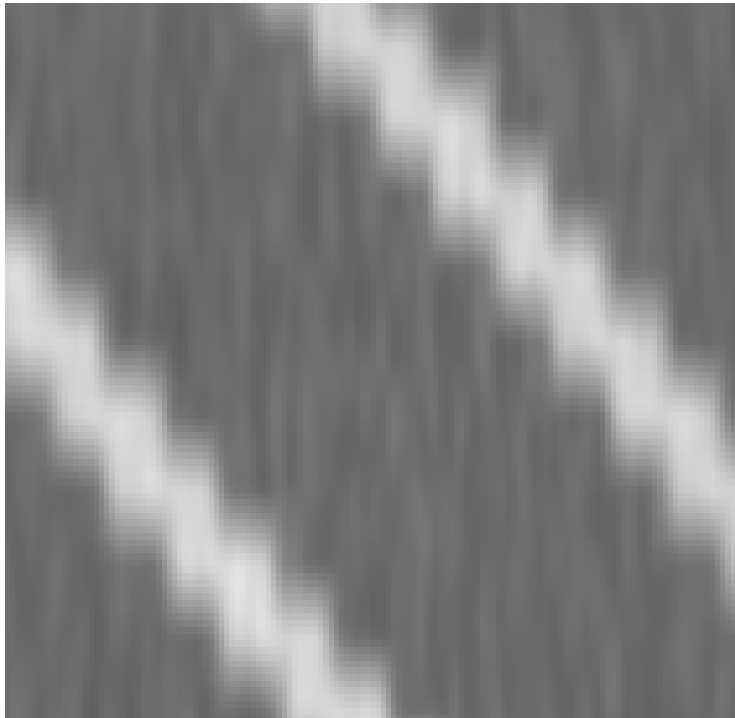
- **Large reconstruction interval**
- **Asymmetric helical interpolation**

Correction

- **Collimation and feed less than feature sizes, and small reconstruction interval**
 - **Adaptive interpolation**
- 



Stair-step Artifacts



(From JA Brink at Yale U)





Metal Artifacts

Cause

Metal blocks parts of projection data

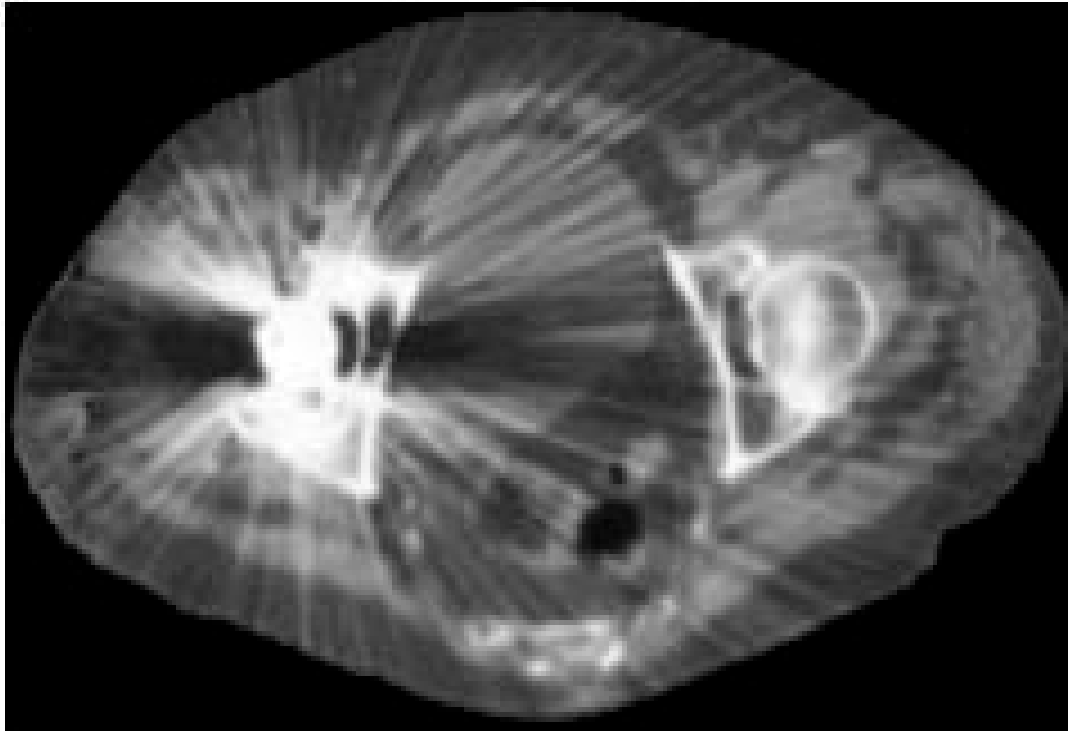
Correction

- **Avoid metal parts**
- **Algorithms**





Metal Artifacts

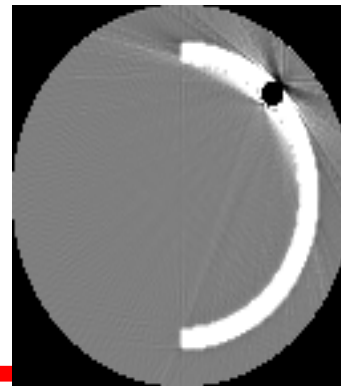
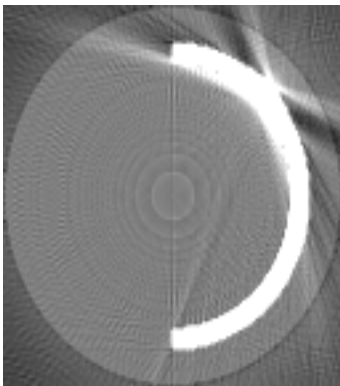


(From DD Robertson at Wash
U)





Metal Artifacts





Motion Artifacts

Causes

Patient motion

Organ motion

heart beating

breathing

swallowing

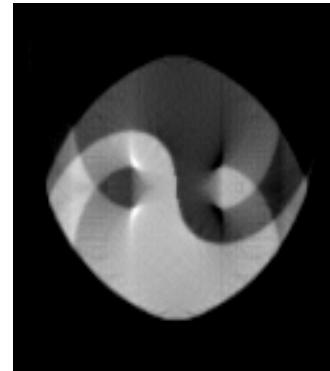
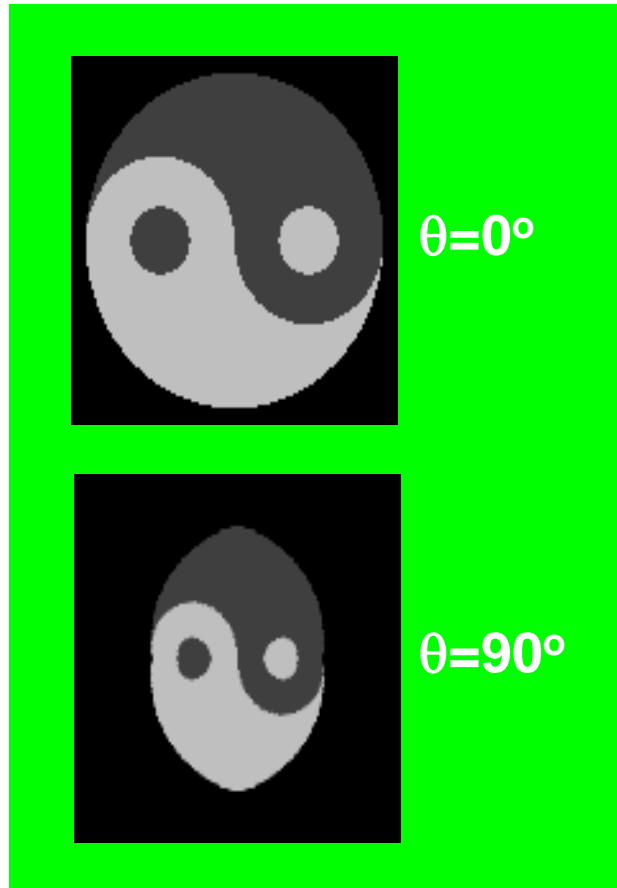
Correction

- **Fast scanning**

- **Algorithms**



Motion Artifacts





Radiation Dose

Dose - radiation energy transferred to an anatomic structure during X-ray scanning

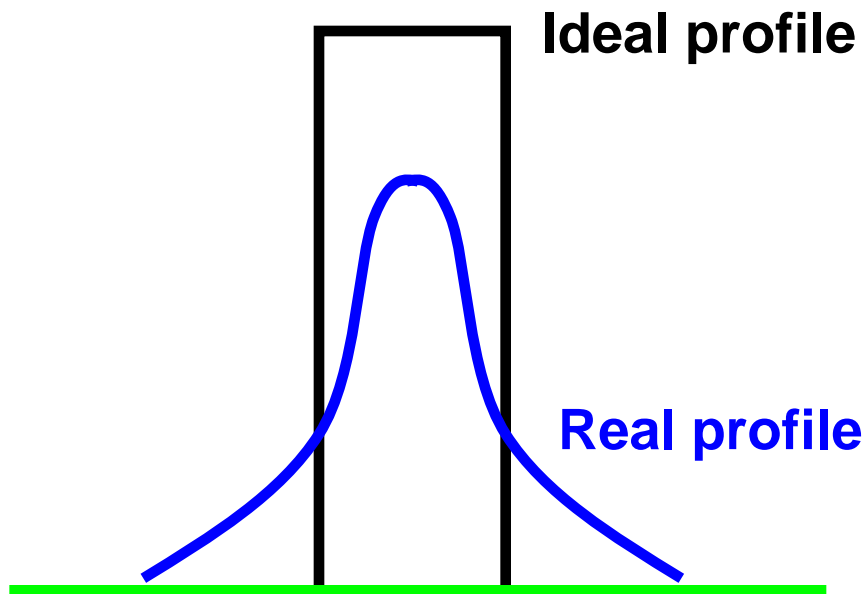
**The unit of dose is Gray (Gy)
sometimes Rad (0.01 Gy)**

Typical values for a CT transaxial scan are in the range of 30 to 50 mGy





Radiation Profile: Single Scan

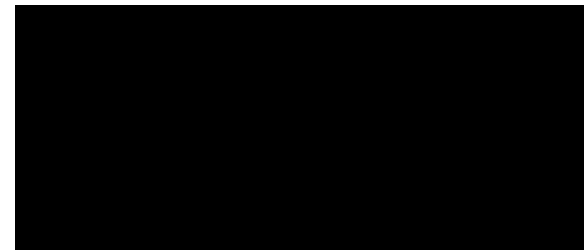
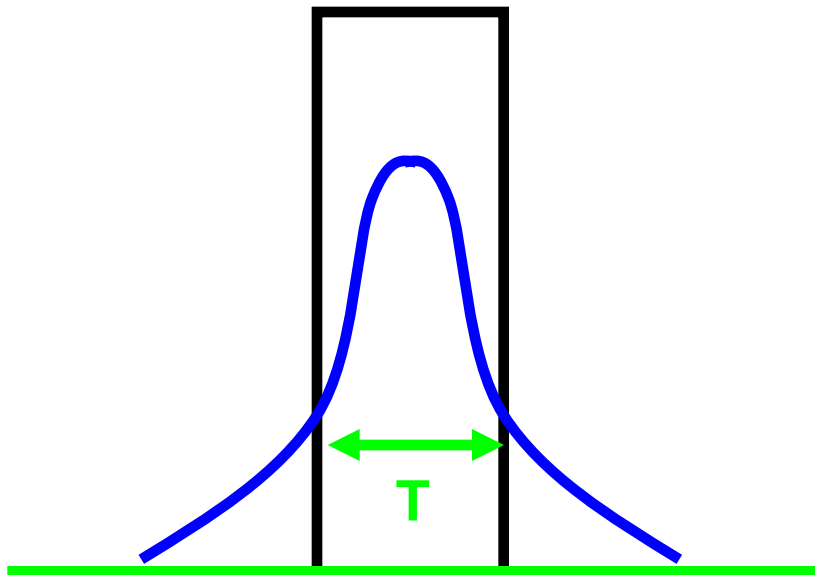


**Radiation spreads outside
the designated slice due to scattering**





CT Dose Index

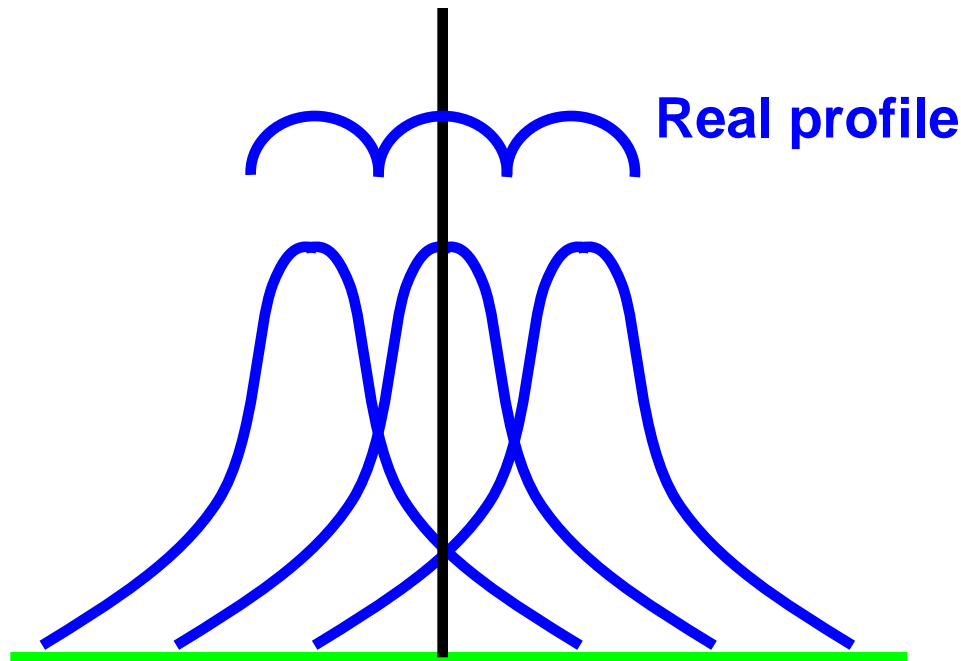


CTDI: CT dose index
T: slice thickness
D(z): local dose
z: longitudinal coordinate





Radiation Profile: Multiple Scans

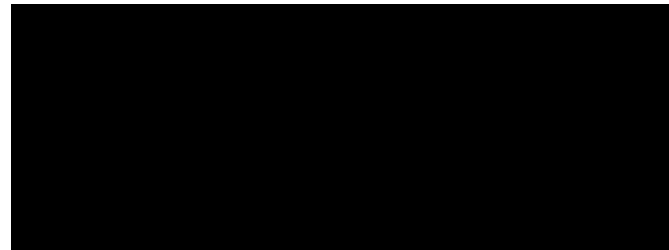
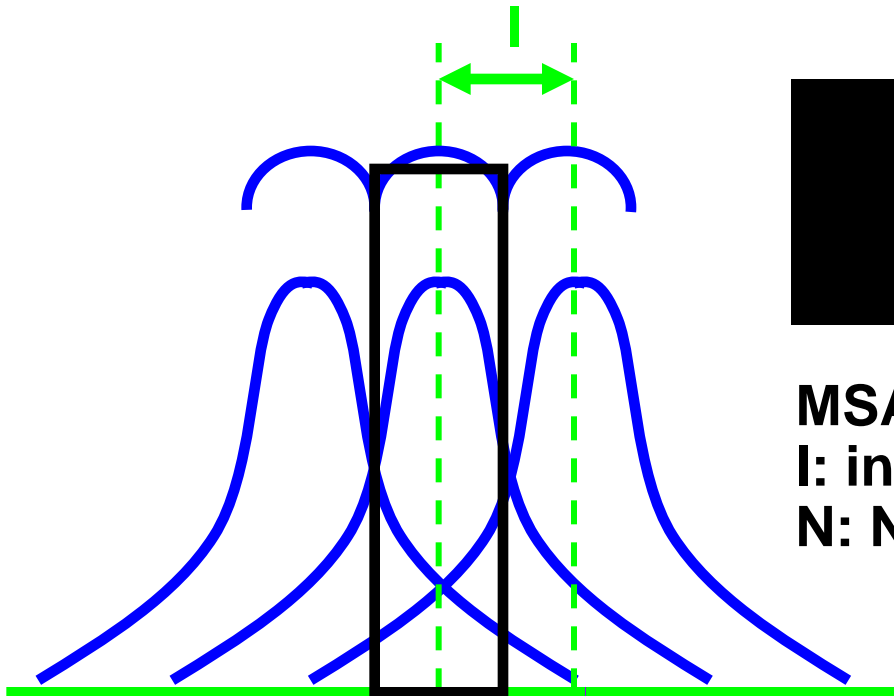


Radiation dose from multiple scans are accumulated in the central slice





Multiple Scan Average Dose

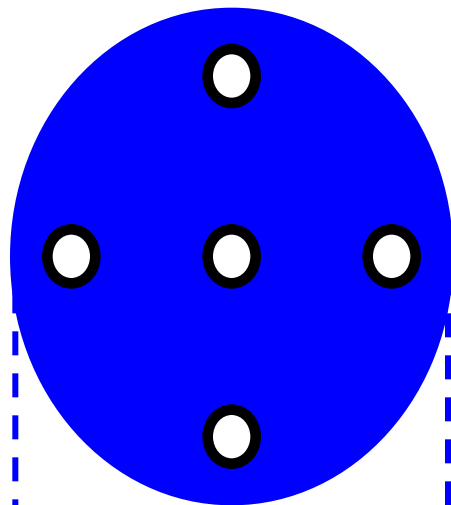


MSAD: multiple scan average dose
l: inter-slice distance
N: Number of scans

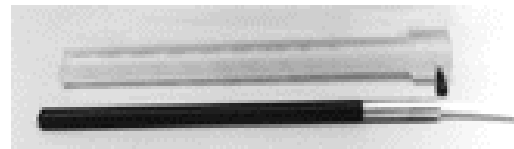


Dose Measurement

- Cylindrical phantoms of 16 cm & 32 cm
- Pencil ionization chamber
- Dosimeter



16 or 32 cm



**PC - 4P CT
PENCIL CHAMBER
Item # 5230 - 2012OPT**



**192 X Digital Dosimeter
Item # 5230 - 3002**



MSAD Estimation

MSAD is

- **directly proportional to mA**
- **directly proportional to scan time**
- **increases with kVp**
 - as compared to dose at 120 kVp
 - 0.2-0.4 times less at 80 kVp
 - 1.2-1.4 times more at 140 kVp
- **increases slightly with decreasing slice thickness**
- **similar at the iso-center and near surface for head**
- **significantly less at the iso-center than near surface for body**

